



南京大學
NANJING UNIVERSITY



Nuclear Matter Properties and Neutron Star Structures from an Extended Linear Sigma Model

Presenter: Yao Ma (马垚)

In collaboration with Prof. Yong-Liang Ma (马永亮)

Hefei, Anhui, May 18th



誠樸雄偉 勵學敦行

Motivation

$$\mathcal{L} = \bar{\psi} \left[i\gamma_{\mu} \partial^{\mu} - M - g_{\sigma} \sigma - g_{\omega} \gamma_{\mu} \omega^{\mu} - g_{\rho} \gamma_{\mu} \tau_a \rho^{a\mu} \right] \psi + \dots$$

The parameterizations in past studies on nuclear matter and neutron stars are lack of considerations of QCD symmetry patterns, such as **chiral symmetry**

Nuclei structures (low/intermediate densities)



- Hadron interactions around saturation density $n_0 = 0.16\text{fm}^{-3}$ are crucial to nuclei structures, e.g. ^{24}Mg , ^{90}Zr , ^{116}Sn and ^{208}Pb

$$E(n, \alpha) = E_0(n) + E_{\text{sym}}(n)\alpha^2 + O(\alpha^4)$$

$$\alpha = (n_n - n_p) / (n_n + n_p)$$

$$E_0(n) = E_0(n_0) + \frac{K_0}{2!}\chi^2 + \frac{J_0}{3!}\chi^3 + O(\chi^4)$$

$$E_{\text{sym}}(n) = E_{\text{sym}}(n_r) + L(n_r)\chi_r + O(\chi_r^2)$$

$$\chi \equiv (n - n_0) / 3n_0$$

$$\mathcal{L} = \bar{\psi} \left[i\gamma_\mu \partial^\mu - M - g_\sigma \sigma - g_\omega \gamma_\mu \omega^\mu - g_\rho \gamma_\mu \tau_a \rho^{a\mu} \right] \psi$$

B. A. Li and C. M. Ko, Nucl. Phys. A 618, 498 (1997).
 D. H. Youngblood, H. L. Clark, and Y. W. Lui, Phys. Rev. Lett. 82, 691 (1999).
 A. W. Steiner and B. A. Li, Phys. Rev. C 72, 041601 (2005).
 L. W. Chen, C. M. Ko, and B. A. Li, Phys. Rev. C 72, 064309 (2005).
 A. E. L. Dieperink, Y. Dewulf, D. Van Neck, M. Waroquier, and V. Rodin, Phys. Rev. C 68, 064307 (2003).
 S. Karataglidis, K. Amos, B. A. Brown, and P. K. Deb, Phys. Rev. C 65, 044306 (2002).
 R. J. Furnstahl, Nucl. Phys. A 706, 85 (2002).
 B. A. Brown, Phys. Rev. Lett. 85, 5296 (2000).

A. Sedrakian, J. J. Li, and F. Weber, Prog. Part. Nucl. Phys. 131, 104041 (2023).
 M. Dutra, et al, Phys. Rev. C 85, 035201 (2012).
 J. M. Lattimer and Y. Lim, Astrophys. J. 771, 51 (2013).
 M. Farine, J. M. Pearson, and F. Tondeur, Nucl. Phys. A 615, 135 (1997).

$$n_0 \rightarrow 0.155 \pm 0.050 (\text{fm}^{-3})$$

$$E_0(n_0) \rightarrow -15.0 \pm 1.0 (\text{MeV})$$

$$E_{\text{sym}}(n_0) \rightarrow 30.9 \pm 1.9 (\text{MeV})$$

$$K_0 \rightarrow 230 \pm 30 (\text{MeV})$$

$$L_0 \rightarrow 52.5 \pm 17.5 (\text{MeV})$$

$$J_0 \rightarrow -700 \pm 500 (\text{MeV})$$

Neutron star (high densities)

The density in the cores of NSs always reach nearly $8n_0$
M-R relations/ tidal deformations are sensitive to the EOS behavior
throughout the whole density regions

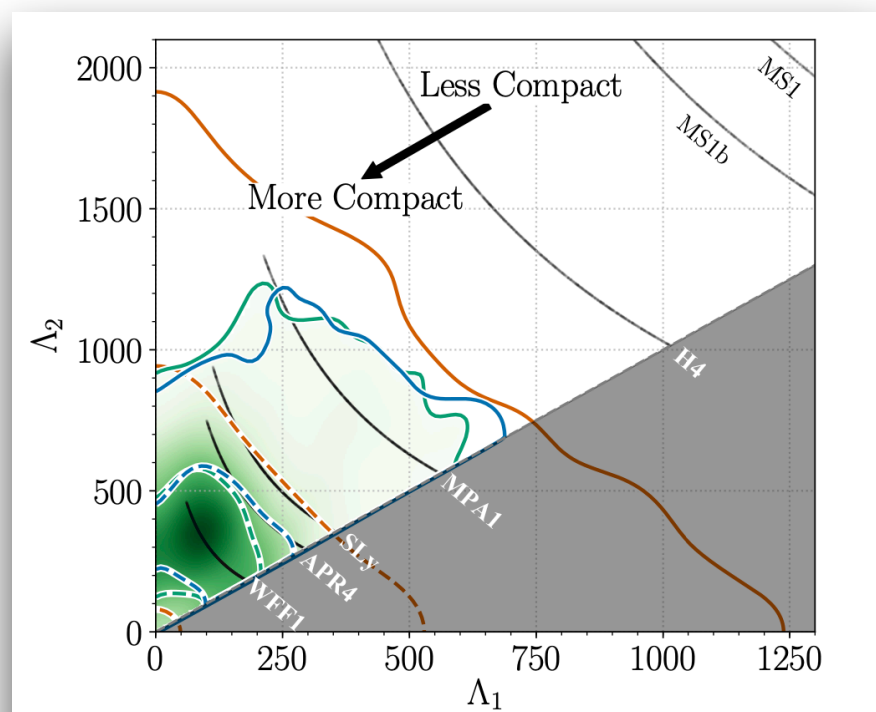


FIG. 1. Marginalized posterior for the tidal deformabilities of the two binary components of GW170817. The green shading shows the posterior obtained using the $\Lambda_a(\Lambda_s, q)$ EOS-insensitive relation to impose a common EOS for the two bodies, while the green, blue, and orange lines denote 50% (dashed) and 90% (solid) credible levels for the posteriors obtained using EOS-insensitive relations, a parametrized EOS without a maximum mass requirement, and independent EOSs (taken from [52]), respectively. The gray shading corresponds to the unphysical region $\Lambda_2 < \Lambda_1$ while the seven black scatter regions give the tidal parameters predicted by characteristic EOS models for this event [113, 115, 121–125].

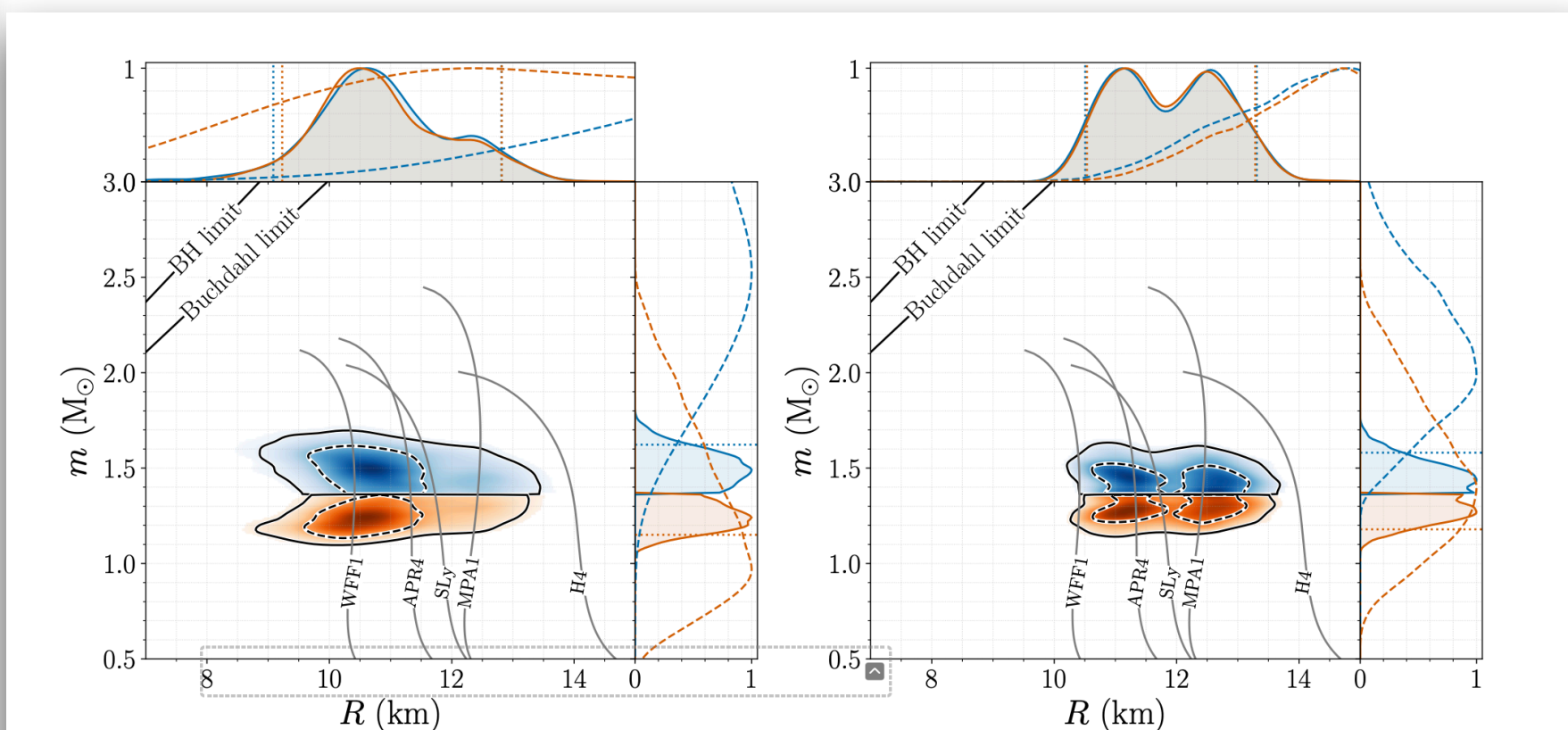


FIG. 3. Marginalized posterior for the mass m and areal radius R of each binary component using EOS-insensitive relations (left panel) and a parametrized EOS where we impose a lower limit on the maximum mass of $1.97 M_\odot$ (right panel). The top blue (bottom orange) posterior corresponds to the heavier (lighter) NS. Example mass-radius curves for selected EOSs are overplotted in gray. The lines in the top left denote the Schwarzschild BH ($R = 2m$) and Buchdahl ($R = 9m/4$) limits. In the one-dimensional plots, solid lines are used for the posteriors, while dashed lines are used for the corresponding parameter priors. Dotted vertical lines are used for the bounds of the 90% credible intervals.

TOV equation

TABLE I. Source properties for GW170817: we give ranges encompassing the 90% credible intervals for different assumptions of the waveform model to bound systematic uncertainty. The mass values are quoted in the frame of the source, accounting for uncertainty in the source redshift.

	Low-spin priors ($ \chi \leq 0.05$)	High-spin priors ($ \chi \leq 0.89$)
Primary mass m_1	$1.36\text{--}1.60 M_\odot$	$1.36\text{--}2.26 M_\odot$
Secondary mass m_2	$1.17\text{--}1.36 M_\odot$	$0.86\text{--}1.36 M_\odot$
Chirp mass \mathcal{M}	$1.188^{+0.004}_{-0.002} M_\odot$	$1.188^{+0.004}_{-0.002} M_\odot$
Mass ratio m_2/m_1	$0.7\text{--}1.0$	$0.4\text{--}1.0$
Total mass m_{tot}	$2.74^{+0.04}_{-0.01} M_\odot$	$2.82^{+0.47}_{-0.09} M_\odot$
Radiated energy E_{rad}	$> 0.025 M_\odot c^2$	$> 0.025 M_\odot c^2$
Luminosity distance D_L	40^{+8}_{-14} Mpc	40^{+8}_{-14} Mpc
Viewing angle Θ	$\leq 55^\circ$	$\leq 56^\circ$
Using NGC 4993 location	$\leq 28^\circ$	$\leq 28^\circ$
Combined dimensionless tidal deformability $\tilde{\Lambda}$	≤ 800	≤ 700
Dimensionless tidal deformability $\Lambda(1.4M_\odot)$	≤ 800	≤ 1400

B. P. Abbott et al. (LIGO Scientific, Virgo), Phys. Rev. Lett. 119, 161101 (2017)
B. P. Abbott et al. (LIGO Scientific, Virgo), Phys. Rev. Lett. 121, 161101 (2018)

Polytropic process + estimations of strong interaction + TOV equation

R. C. Tolman, Phys. Rev. 55, 364 (1939).

J. R. Oppenheimer and G. M. Volkoff, Phys. Rev. 55, 374 (1939).

δ meson effects

T. Miyatsu, M.-K. Cheoun, and K. Saito, *Astrophys. J.* 929, 82 (2022).

$$\tilde{g}_{\sigma^2\delta^2}\sigma^2\vec{\delta}^2 \quad \tilde{g}_{\sigma\delta^2}\sigma\vec{\delta}^2 \quad g_{\delta}\vec{\delta}\vec{\psi}\vec{\tau}\vec{\psi}$$

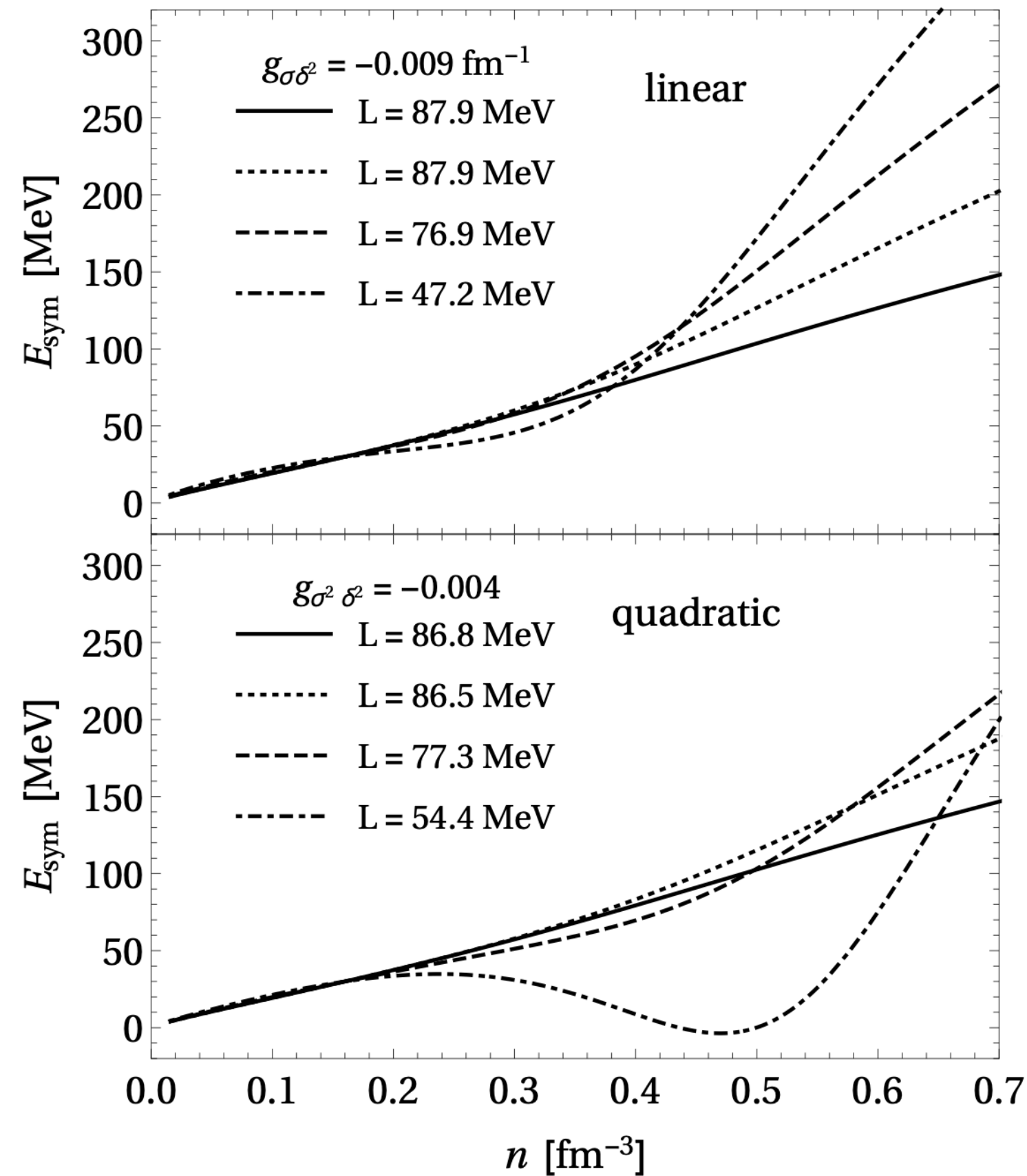


FIG. 2. Symmetry energy E_{sym} for negative value of g_{α} with respect to various values of C_{δ}^2 for both types of coupling.

N. Zabari, S. Kubis, and W. Wójcik, *Phys. Rev. C* 99, 035209 (2019).

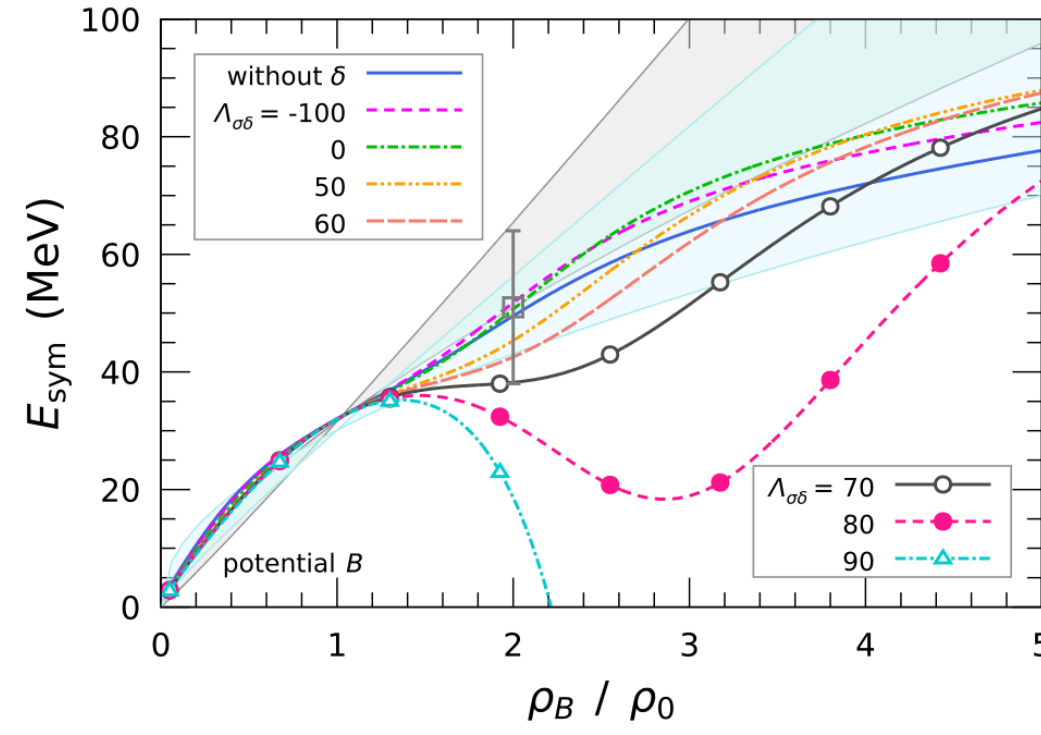


Figure 4. Same as Figure 3 but with the σ - δ mixing. The coupling constants in potential B are used.

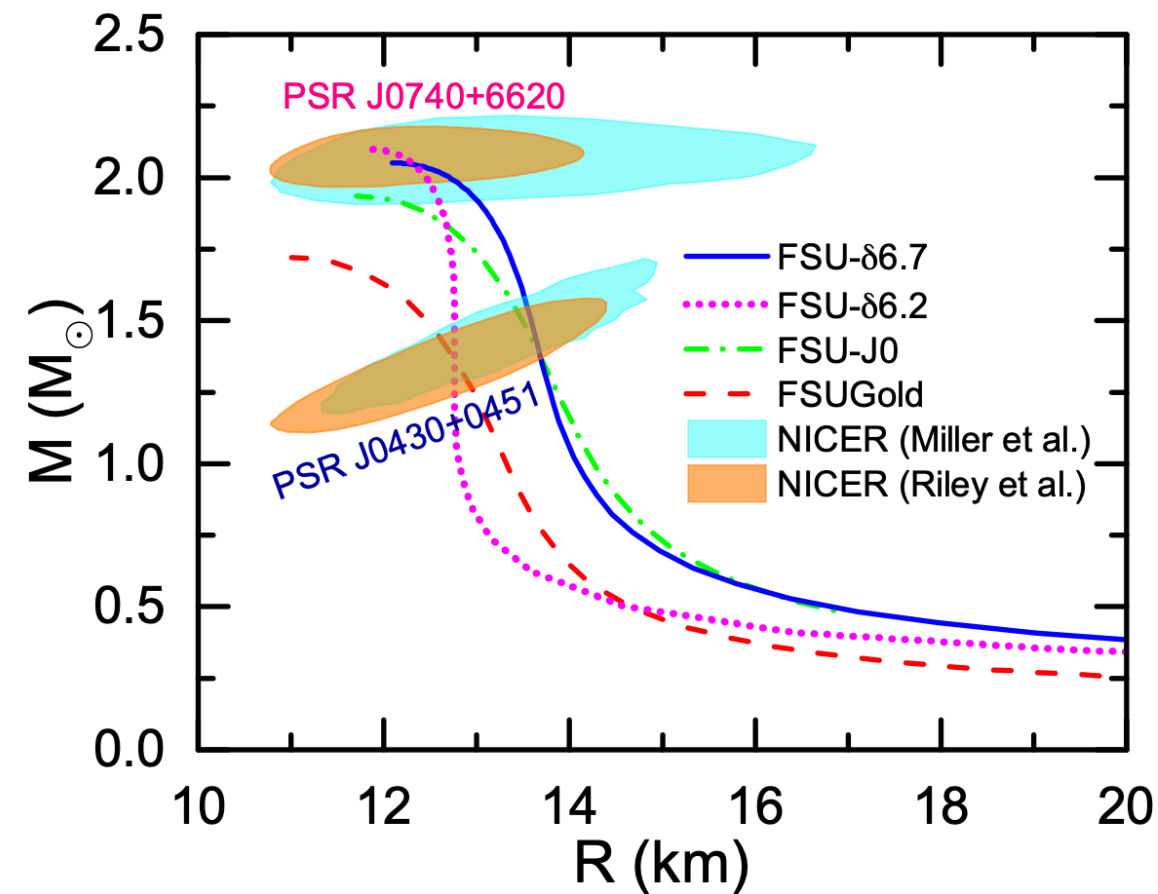


Figure 2. M-R relation for static NSs from FSUGold, FSU-J0, FSU- δ 6.7 and FSU- δ 6.2. The NICER (XMM-Newton) constraints with 68% C.L for PSR J0030+0451 (Riley et al. 2019; Miller et al. 2019) and PSR J0740+6620 (Riley et al. 2021; Miller et al. 2021) are also included for comparison.

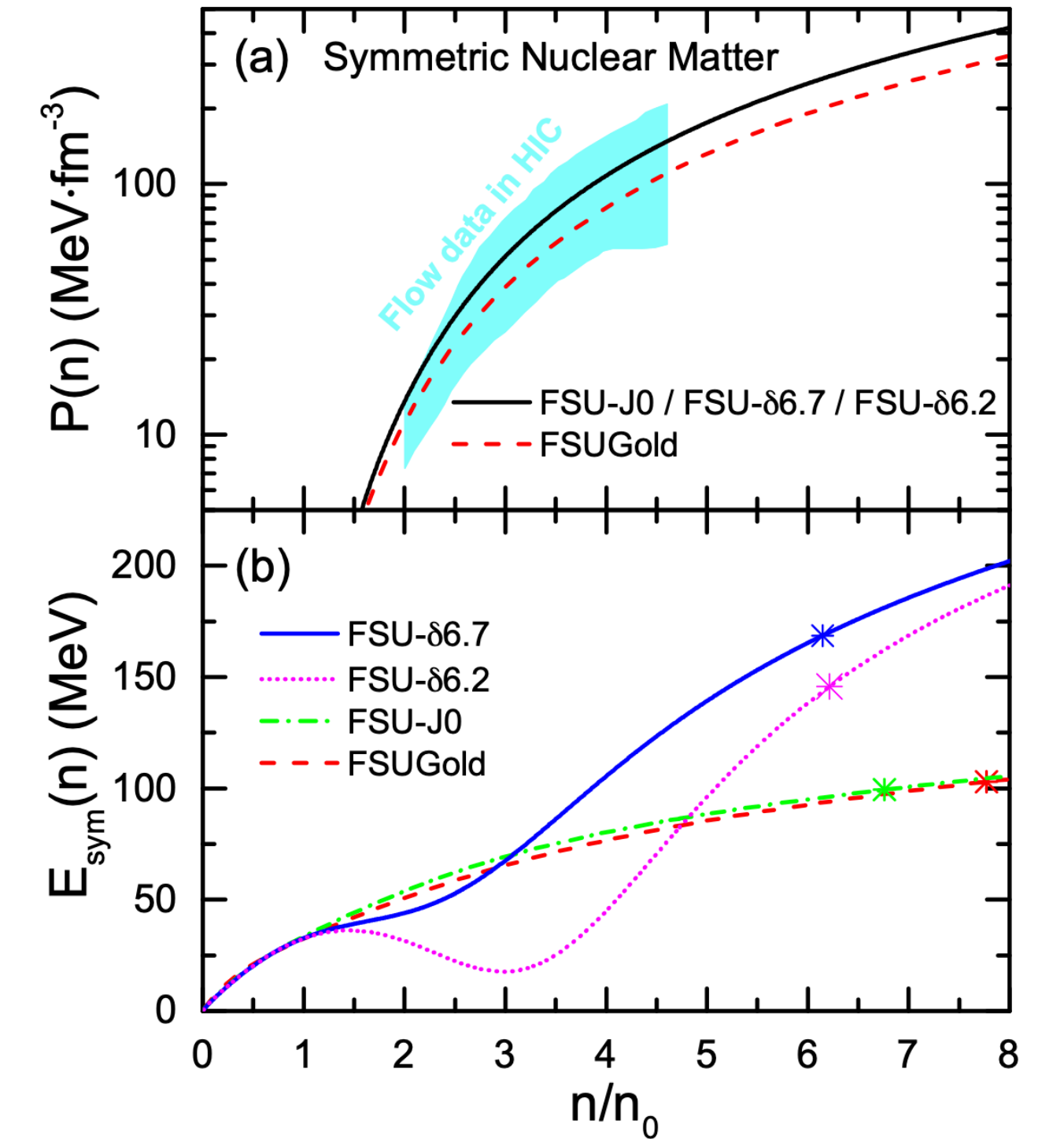
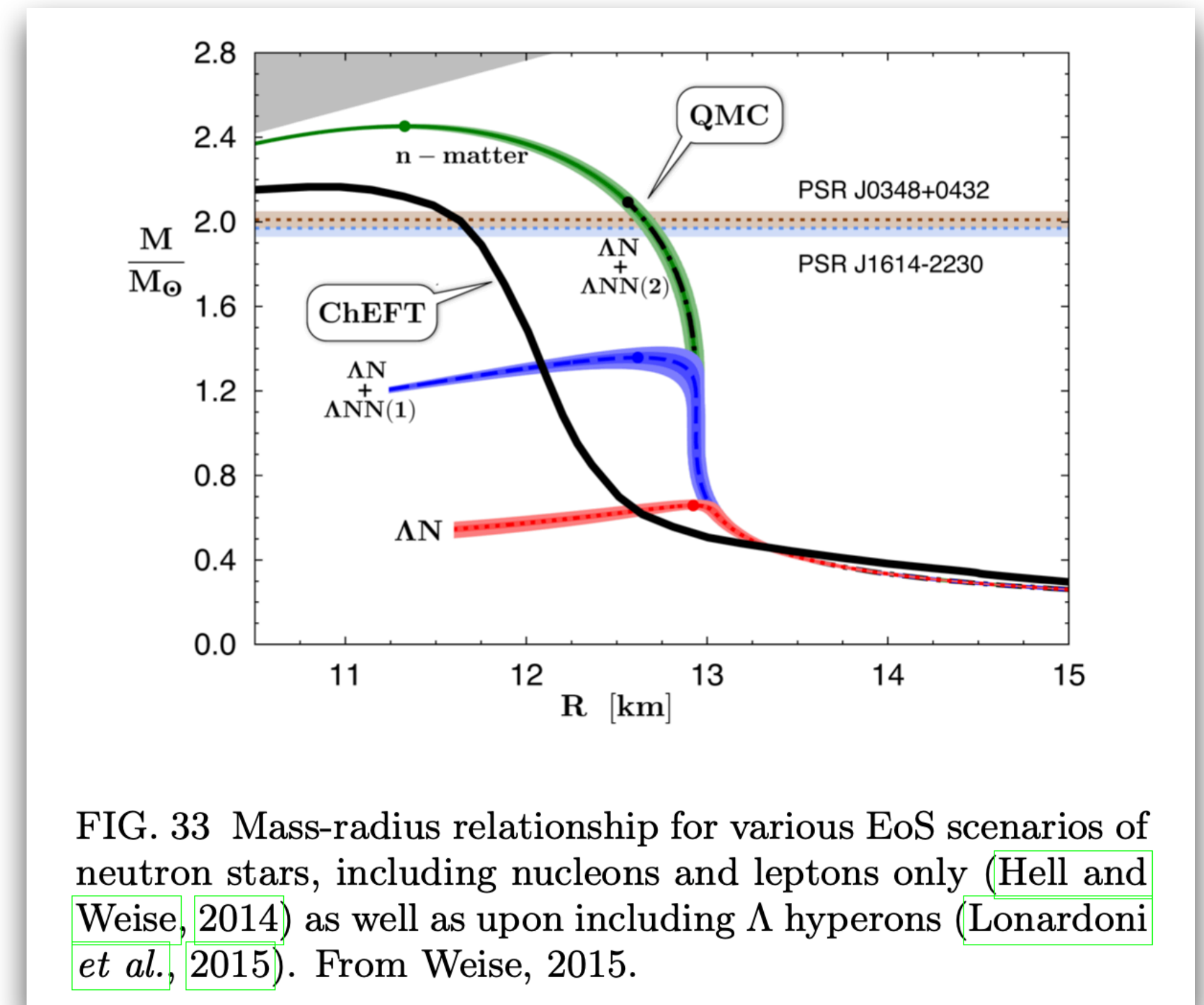
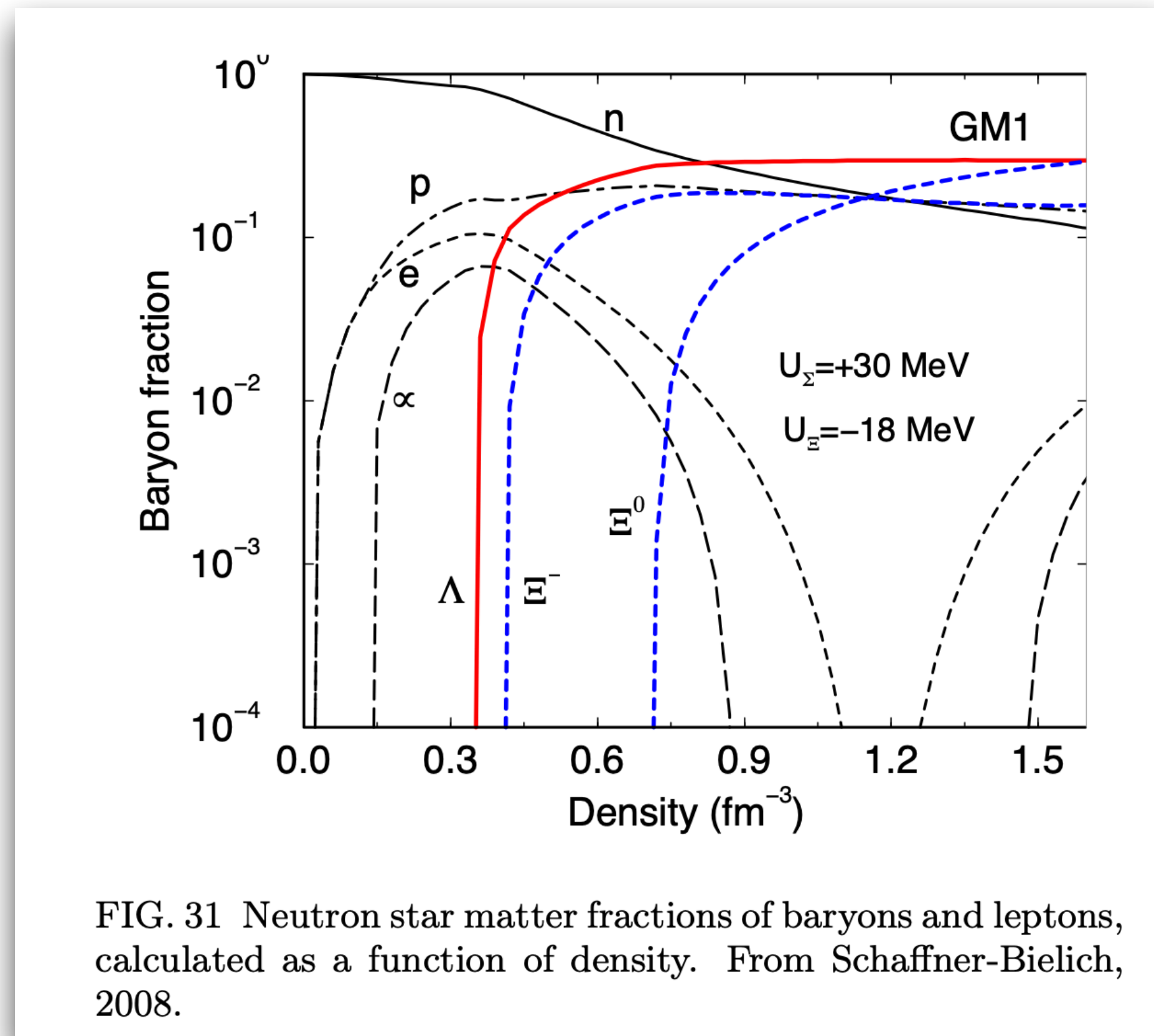


Figure 1. Pressure vs density (a) and density dependence of the symmetry energy (b) predicted by FSUGold, FSU-J0, FSU- δ 6.7 and FSU- δ 6.2. The shaded area in panel (a) represents the constraints from flow data in heavy-ion collisions (Danielewicz et al. 2002). The central density of maximum mass NS configuration is indicated by ‘*’ in panel (b).

F. Li, B.-J. Cai, Y. Zhou, W.-Z. Jiang, and L.-W. Chen, *Astrophys. J.* 929, 183 (2022).

Hyperon effects (Strangeness)

$$\mathcal{L}_b = \sum_b \bar{\psi}_b \left[\gamma^\mu \left(i\partial_\mu - g_{\omega b} \omega_\mu - g_{\rho b} \tau_b \cdot \rho_\mu \right) - \left(m_b - g_{\sigma b} \sigma \right) \right] \psi_b$$



Chemical potential equilibrium, e.g. $\mu_\Lambda = \mu_p + \mu_e$

A. Gal, E. V. Hungerford, and D. J. Millener, *Rev. Mod. Phys.* 88, 035004 (2016).

Method to handle dense system



1. Relativistic mean field approximation

J. D. Walecka, Ann. Phys. 83, 491 (1974).

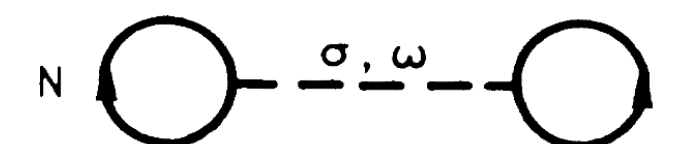
$$\begin{aligned} \mathcal{L} &= \mathcal{L}_N + \mathcal{L}_\sigma + \mathcal{L}_\omega + \mathcal{L}_I \\ \mathcal{L}_N &= \bar{\psi} \left(i\gamma_\mu \partial^\mu - m_N \right) \psi \\ \mathcal{L}_\sigma &= \frac{1}{2} \left(\partial_\mu \phi \partial^\mu \phi - m_\sigma^2 \phi^2 \right) \\ \mathcal{L}_\omega &= -\frac{1}{4} W_{\mu\nu} W^{\mu\nu} + \frac{1}{2} m_\omega^2 \omega_\mu \omega^\mu \\ \mathcal{L}_I &= \mathcal{L}_{\sigma N} + \mathcal{L}_{\omega N} = g_\sigma \phi \bar{\psi} \psi - g_\omega \omega^\mu \bar{\psi} \gamma_\mu \psi \end{aligned}$$

$$\begin{aligned} \left(i\gamma_\mu \partial^\mu - g_\omega \gamma_0 \omega^0 - m_N \right) \psi &= 0, \quad m_N^* = m_N - g_\sigma \phi, \\ \phi &= \frac{g_\sigma}{m_\sigma^2} \rho_s, \quad \rho_s = \langle \bar{\psi} \psi \rangle, \\ \omega^0 &= \frac{g_\omega}{m_\omega^2} \rho_B, \quad \rho_B = \langle \psi^\dagger \psi \rangle, \end{aligned}$$

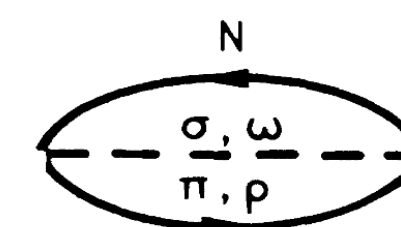
2. Relativistic Hartree-Fock method

$$\begin{aligned} \mathcal{L}_I &= -g_\sigma \bar{\psi} \psi - g_\omega \bar{\psi} \gamma_\mu \omega^\mu \psi + \frac{f_\omega}{2M} \bar{\psi} \sigma_{\mu\nu} \partial^\nu \omega^\mu \psi \\ &\quad - g_\rho \bar{\psi} \gamma_\mu \rho^\mu \cdot \tau \psi + \frac{f_\rho}{2M} \bar{\psi} \sigma_{\mu\nu} \partial^\nu \rho^\mu \cdot \tau \psi \\ &\quad - e \bar{\psi} \gamma_\mu \frac{1}{2} (1 + \tau_3) A^\mu \psi + \mathcal{L}_{\pi NN} \end{aligned}$$

$$\Sigma(\mathbf{p}) = \Sigma_S(p) + \gamma_0 \Sigma_0(p) + \boldsymbol{\gamma} \cdot \hat{\mathbf{p}} \Sigma_V(p)$$



(a)



(b)

A. Bouyssy, J.-F. Mathiot, N. V. Giai, and S. Marcos, Phys Rev C 36, 380 (1987).



誠樸雄偉 勵學敦行

Can we extend an EFT/model taking care of QCD symmetry patterns into dense nucleon systems?

An extended linear sigma model in nuclear matter

Phys. Rev. D 109 (2024) 7, 7, YM and Y. L. Ma

Phys. Rev. D 112 (2025) 5, 054026, YM and Y. L. Ma

P-wave problems in light scalar meson sectors below 1 GeV



F. E. Close and N. A. Tornqvist, J. Phys. G 28, R249 (2002)

A tetra-quark picture to include δ ($a_0(980)$) meson and hyperon



Freedoms to be considered

Highlights of the parametrization:

- I. Include meson exchanges, e.g. $f_0(500)(\sigma)$ and $a_0(980)(\delta)$
- II. Include baryon freedoms, e.g. nucleon and hyperon

$$\sigma = \cos \theta_0 \sigma' + \sin \theta_0 \hat{\sigma}'$$

$$a_0 = \cos \theta_8 a_0' + \sin \theta_8 \hat{a}_0'$$

$$f_0 = \cos \theta_8 f_0' + \sin \theta_8 \hat{f}_0'$$

$$R^\mu = V^\mu - A^\mu = \frac{1}{\sqrt{2}} \begin{pmatrix} \frac{\omega_N^\mu + \rho^{\mu 0}}{\sqrt{2}} - \frac{f_{1N}^\mu + a_1^{\mu 0}}{\sqrt{2}} & \rho^{\mu+} - a_1^{\mu+} & K^{*\mu+} - K_1^{\mu+} \\ \rho^{\mu-} - a_1^{\mu-} & \frac{\omega_N^\mu - \rho^{\mu 0}}{\sqrt{2}} - \frac{f_{1N}^\mu - a_1^{\mu 0}}{\sqrt{2}} & K^{*\mu 0} - K_1^{\mu 0} \\ K^{*\mu-} - K_1^{\mu-} & \bar{K}^{*\mu 0} - \bar{K}_1^{\mu 0} & \omega_S^\mu - f_{1S}^\mu \end{pmatrix}$$

$$L^\mu = V^\mu + A^\mu = \frac{1}{\sqrt{2}} \begin{pmatrix} \frac{\omega_N^\mu + \rho^{\mu 0}}{\sqrt{2}} + \frac{f_{1N}^\mu + a_1^{\mu 0}}{\sqrt{2}} & \rho^{\mu+} + a_1^{\mu+} & K^{*\mu+} + K_1^{\mu+} \\ \rho^{\mu-} + a_1^{\mu-} & \frac{\omega_N^\mu - \rho^{\mu 0}}{\sqrt{2}} + \frac{f_{1N}^\mu - a_1^{\mu 0}}{\sqrt{2}} & K^{*\mu 0} + K_1^{\mu 0} \\ K^{*\mu-} + K_1^{\mu-} & \bar{K}^{*\mu 0} + \bar{K}_1^{\mu 0} & \omega_S^\mu + f_{1S}^\mu \end{pmatrix}$$

$$\Phi = S + iP = \begin{pmatrix} \frac{(\sigma_N + a_0^0) + i(\eta_N + \pi^0)}{\sqrt{2}} & a_0^+ + i\pi^+ & K_S^+ + iK^+ \\ a_0^- + i\pi^- & \frac{(\sigma_N - a_0^0) + i(\eta_N - \pi^0)}{\sqrt{2}} & K_S^0 + iK^0 \\ K_S^- + iK^- & \bar{K}_S^0 + i\bar{K}^0 & \sigma_S + i\eta_S \end{pmatrix}$$

$$\langle \sigma' \rangle = \sqrt{3}\alpha \text{ and } \langle \hat{\sigma}' \rangle = \sqrt{3}\beta$$

a_0 mesons may be crucial to NS tidal deformations and neutron skin of nucleus

$$B_N \equiv \begin{pmatrix} \frac{\Lambda}{\sqrt{6}} + \frac{\Sigma^0}{\sqrt{2}} & \Sigma^+ & p \\ \Sigma^- & \frac{\Lambda}{\sqrt{6}} - \frac{\Sigma^0}{\sqrt{2}} & n \\ \Xi^- & \Xi^0 & -\frac{2\Lambda}{\sqrt{6}} \end{pmatrix}$$

High densities may lead to hyperon cores of NSs

D. Adhikari et al. (PREX), Phys. Rev. Lett. 126, 172502 (2021)

B. T. Reed, F. J. Fattoyev, C. J. Horowitz, and J. Piekarewicz, Phys. Rev. Lett. 126, 172503 (2021)

F. Li, B. J. Cai, Y. Zhou, W. Z. Jiang, and L. W. Chen, Astrophys. J. 929, 183 (2022)

N. K. Glendenning, Astrophys. J. 293, 470 (1985)

N. K. Glendenning and S. A. Moszkowski, Phys. Rev. Lett. 67, 2414 (1991).

S. Weissenborn, D. Chatterjee, and J. Schaffner-Bielich, Phys. Rev. C 85, 065802 (2012), [Erratum: Phys. Rev. C 90, 019904 (2014)]

The chiral transformations



$$SU(3)_R \otimes SU(3)_L$$

$$\begin{aligned} \Phi' &\rightarrow g_L \Phi' g_R^\dagger, & \hat{\Phi}' &\rightarrow g_L \hat{\Phi}' g_R^\dagger \\ L_\mu &\rightarrow g_L L_\mu g_L^\dagger, & R_\mu &\rightarrow g_R R_\mu g_R^\dagger \\ N_R^{(RR)} &\rightarrow g_R N_R^{(RR)} g_R^\dagger \\ N_R^{(LL)} &\rightarrow g_R N_R^{(LL)} g_L^\dagger \end{aligned}$$

Scalars Vectors Baryons

$$\begin{aligned} \Phi' &\rightarrow e^{2iv} \Phi', & \hat{\Phi}' &\rightarrow e^{-4iv} \hat{\Phi}', \\ L_\mu &\rightarrow L_\mu, & R_\mu &\rightarrow R_\mu \\ N_R^{(RR)} &\rightarrow e^{-3iv} N_R^{(RR)}, & N_L^{(RR)} &\rightarrow e^{-iv} N_L^{(RR)} \\ N_R^{(LL)} &\rightarrow e^{iv} N_R^{(LL)}, & N_L^{(LL)} &\rightarrow e^{3iv} N_L^{(LL)} \end{aligned}$$

di-quark approximation

Power counting rules



- ① The operators are limited **within dimension-4**, for the higher dimensional operators are suppressed by the cutoff scale;
- ② The **quark number** of an operator is limited within 8 and the number of flavor space traces is limited to only 1, for its suppression by N_c ;
- ③ The **explicit symmetry** breaking caused by quark mass is treated as **perturbation**, which is crucial to strangeness in NS.

A. H. Fariborz, R. Jora, and J. Schechter, Phys. Rev. D 77, 034006 (2008).
A. H. Fariborz, R. Jora, and J. Schechter, Phys. Rev. D 72, 034001 (2005)
A. H. Fariborz, R. Jora, and J. Schechter, Phys. Rev. D 79, 074014 (2009)
D. Parganlija, F. Giacosa, and D. H. Rischke, Phys. Rev. D 82, 054024 (2010)

The Lagrangian at the leading order for RMF



$$\mathcal{V}_M = c_2 \text{Tr} S'^2 - d_2 \text{Tr} \hat{S}'^2 - c_4 \text{Tr} S'^4 - 2e_3 \epsilon_{abc} \epsilon_{def} S'_{ad} S'_{be} \hat{S}'_{cf}$$

Quark configuration mixing

$$\mathcal{V}_V = \tilde{h}_2 \text{Tr} (S'^2 V^2) + \tilde{g}_3 \text{Tr} V^4 +$$

$$a_1 \epsilon_{abc} \epsilon_{def} V_{ad} V_{be} (S'^2)_{cf}$$

Masses by spontaneous chiral symmetry breaking

$$\mathcal{L}_B^{\text{RMF}} = \text{Tr} \left(\bar{B} i \gamma_\mu \partial^\mu B \right) + c \text{Tr} \left(\bar{B} \gamma^0 V B \right) - g \text{Tr} \left(\bar{B} S' B \right)$$

$$+ h \epsilon_{abc} \epsilon_{def} \bar{B}_{ad} \gamma^0 B_{be} V_{cf}$$

$$- e \epsilon_{abc} \epsilon_{def} \bar{B}_{ad} \gamma^0 B_{be} S'_{cf}$$

Only two quark configuration couples to baryon at the leading order

Hadron masses and NM properties

The units are in MeV, except n_0 is in fm^{-3}

Y. Sugahara and H. Toki, Nucl. Phys. A579,557 (1994).
 F. Li, B. J. Cai, Y. Zhou, W. Z. Jiang, and L. W. Chen, Astrophys. J. 929, 183 (2022).

	$g_{\sigma NN}$	$g_{a_0 NN}$	$g_{f NN}$	$g_{\omega NN}$	$g_{\rho NN}$
TM1	-10.0	—	—	-12.6	-4.63
FSU- $\delta 6.7$	10.2	6.7	—	-13.4	-7.27
el-g30g	-6.17	5.13	2.95	-6.09	5.30
el-g30e	-6.20	-5.03	3.00	6.09	5.30
el-g30eg	-5.97	-0.671	2.68	6.06	3.45
el-g350eg	-6.12	-0.852	2.85	6.37	3.71
el-g3100eg	-6.36	-0.442	3.19	6.73	3.85
el-g3150eg	-6.38	-0.413	3.20	7.09	4.04

Increasing the four-vector couplings



	n_0	E_0	$E_{\text{sym}}(n_0)$	$J(n_0)$	$L(n_0)$	$K(n_0)$
Empirical	0.155 ± 0.050	-16.0 ± 1.0	31.7 ± 3.2	-200 ± 600	58.7 ± 28.1	250 ± 50
el-g30g	0.155	-14.6	30.9	451	83.6	418
el-g30e	0.155	-14.6	31.6	479	85.8	419
el-g30eg	0.155	-14.6	30.1	421	82.2	415
el-g350eg	0.155	-15.2	30.9	-392	80.7	370
el-g3100eg	0.155	-15.4	31.4	-1020	71.7	317
el-g3150eg	0.155	-15.6	31.6	-1470	63.7	253

	m_N	m_σ	$m_{f_0(a_0)}$	$m_{f_0(a'_0)}$	$m_{\sigma'}$	m_ρ	m_ρ
Empirical	938-940	400-800	960-1010	1250-1500	1430-1530	761-765	782-783
el-g30g	939	522	989	1480	1510	763	783
el-g30e	939	525	991	1480	1510	763	783
el-g30eg	939	498	983	1500	1520	763	783
el-g350eg	939	485	991	1470	1510	763	783
el-g3100eg	939	502	994	1470	1510	763	783
el-g3150eg	939	485	991	1470	1510	763	783

A. Sedrakian, J. J. Li, and F. Weber, Prog. Part. Nucl. Phys. 131, 104041 (2023)
 J. Piekarewicz, Phys. Rev. C 69, 041301 (2004).
 M.I. Tews, J. M. Lattimer, A. Ohnishi, and E. E. Kolomeitsev, Astrophys. J. 848, 105 (2017).
 M. Dutra, et al., Phys. Rev. C 85, 035201 (2012).
 R. L. Workman, et al. (Particle Data Group), PTEP 2022, 083C01 (2022).

Comparison with Walecka-type models

Saturation density

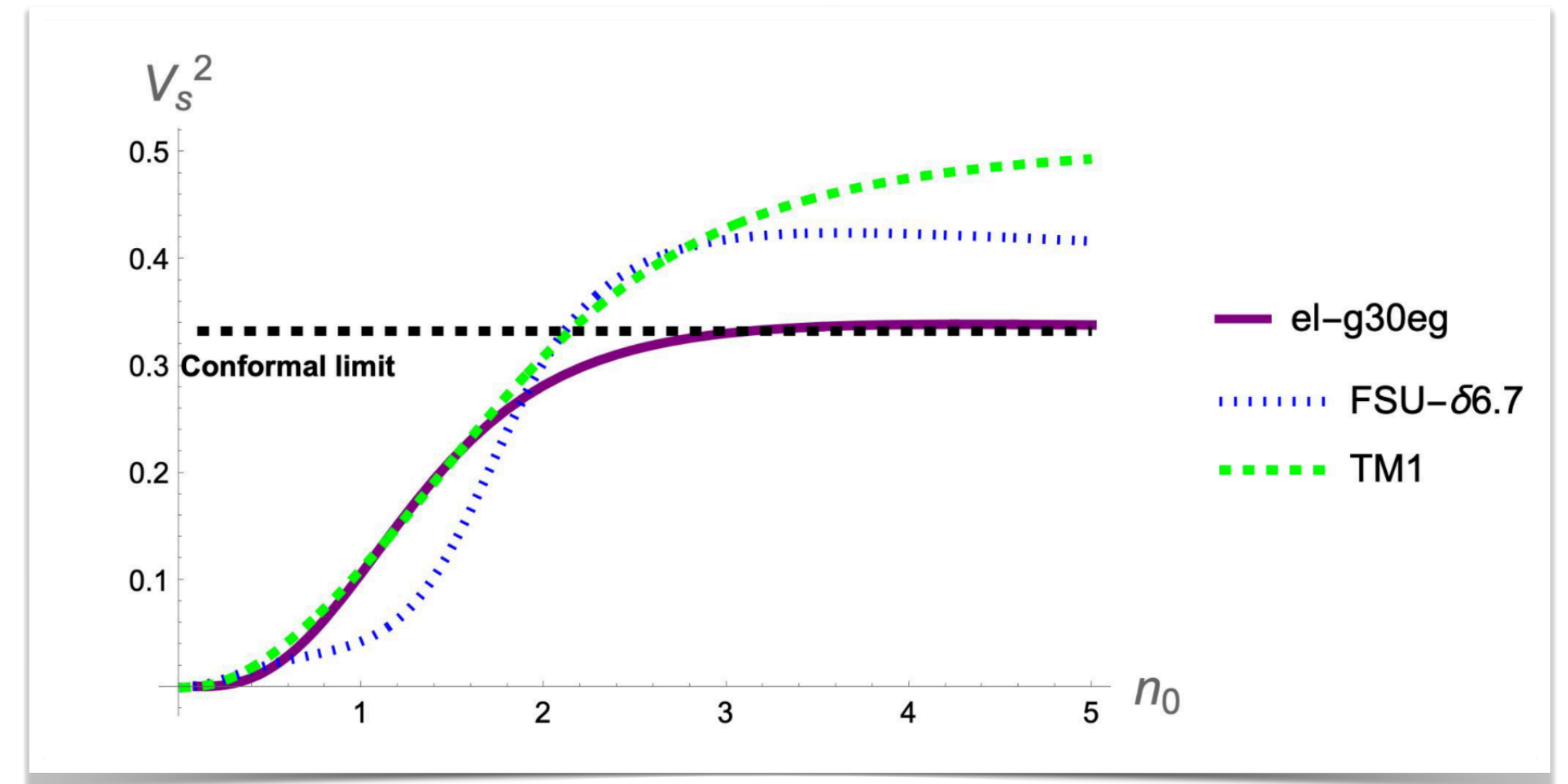
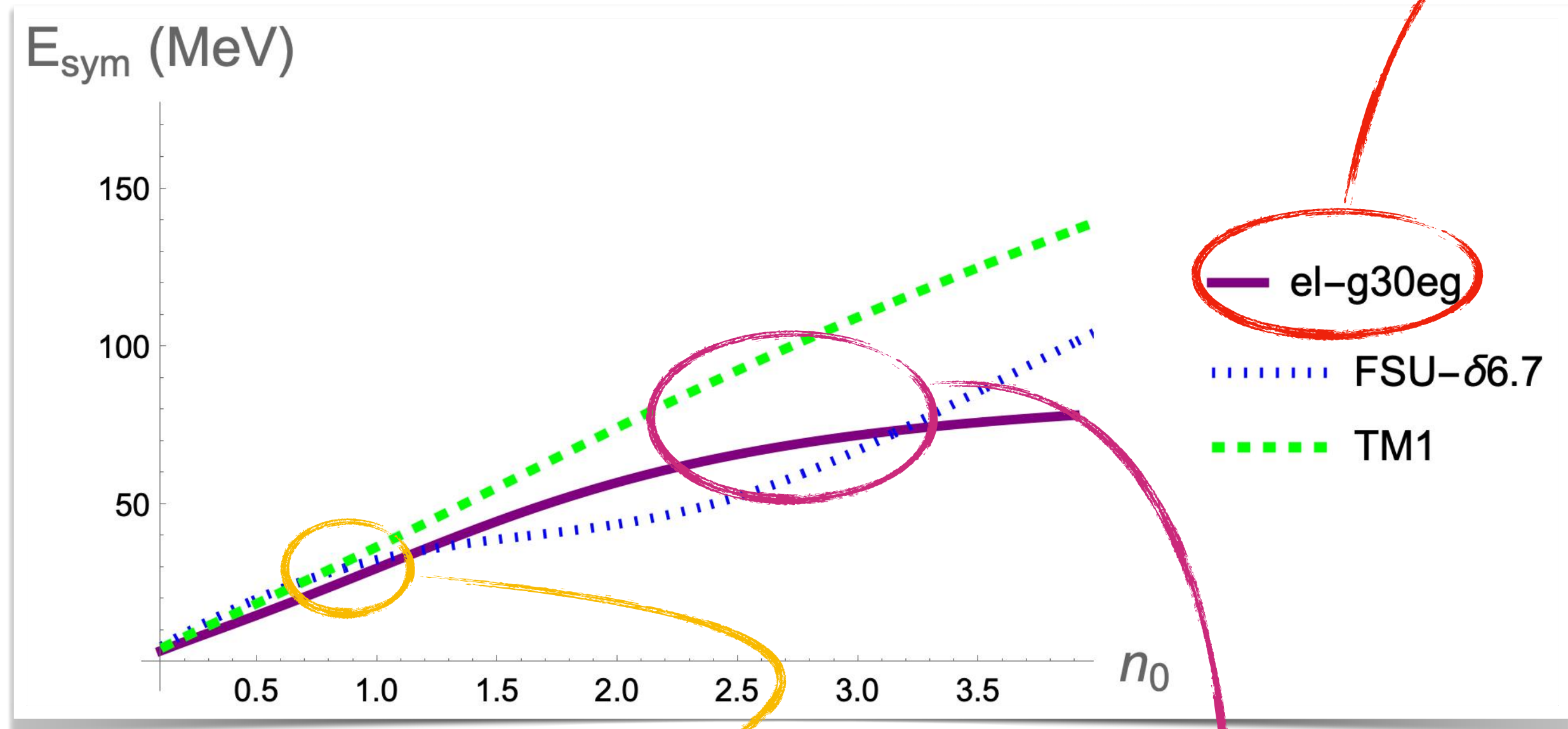
A. Sedrakian, J. J. Li, and F. Weber, Prog. Part. Nucl. Phys. 131, 104041 (2023)

	Empirical	ELSM	TM1	FSU – $\delta 6.7$
$n_0(\text{fm}^{-3})$	0.155 ± 0.005	0.155	0.145	0.148

Small g_3 and g_δ

Symmetric nuclear matter

Pure neutron matter

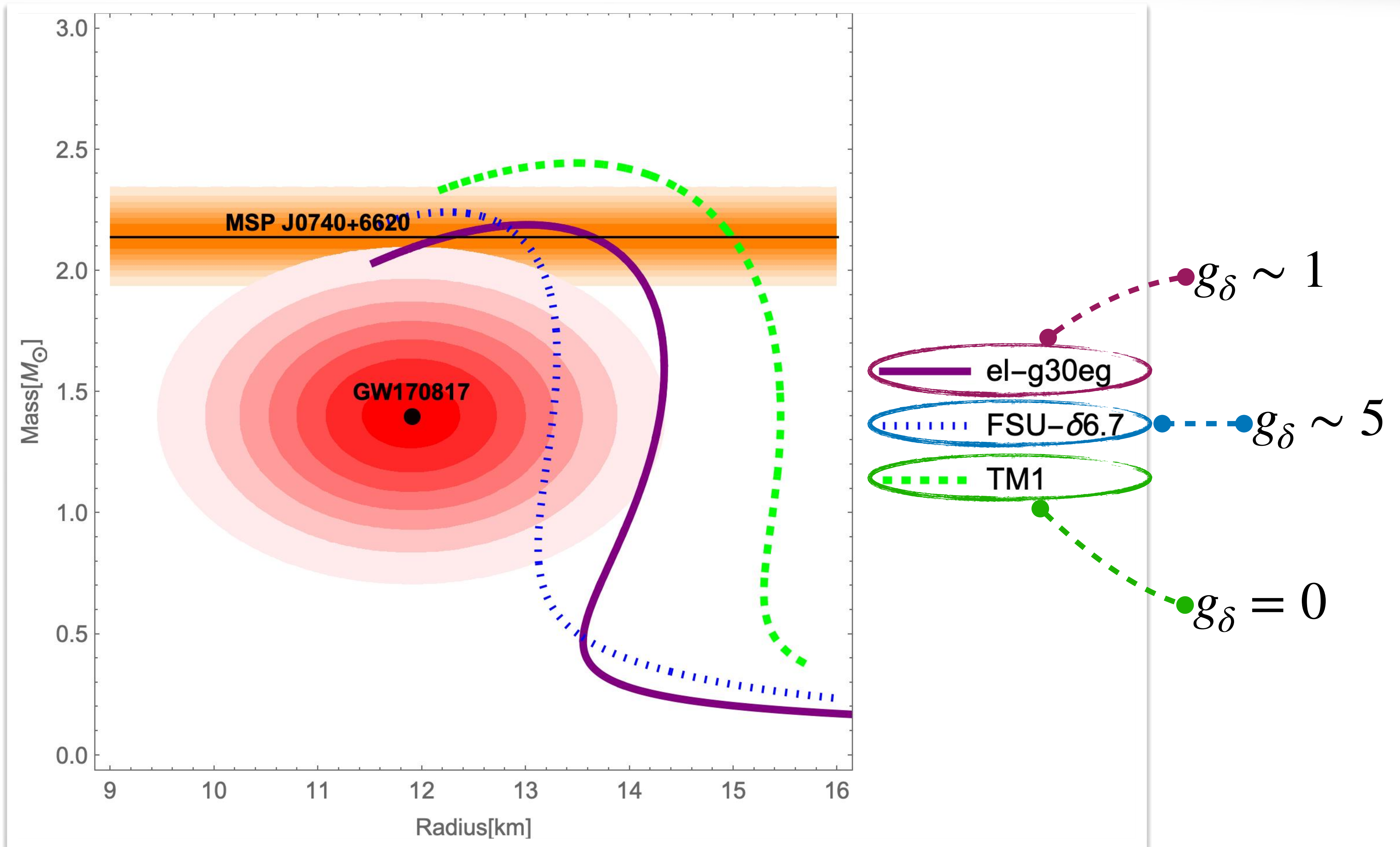


$L(2/3n_0) \geq 49 \text{ MeV}$

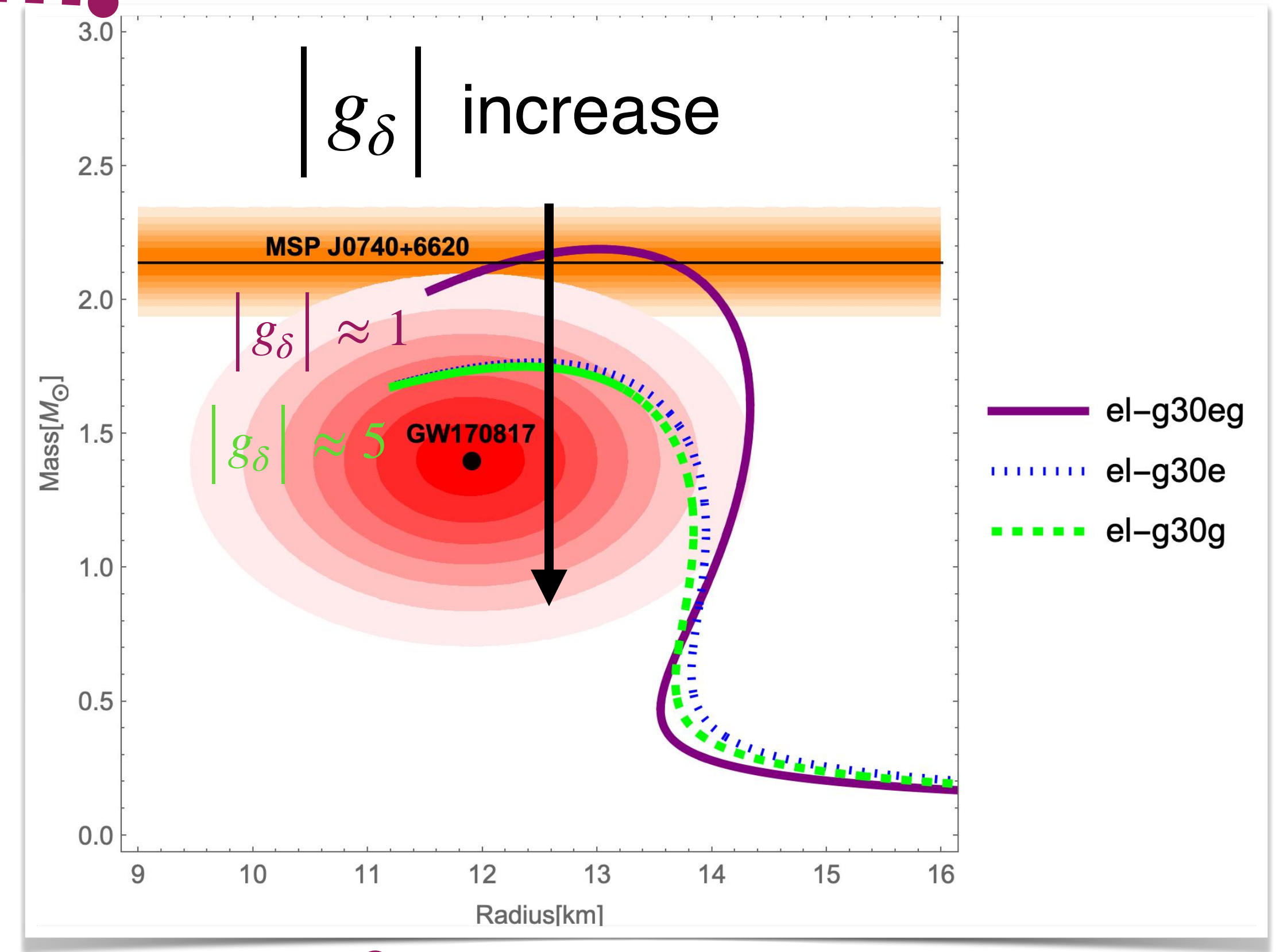
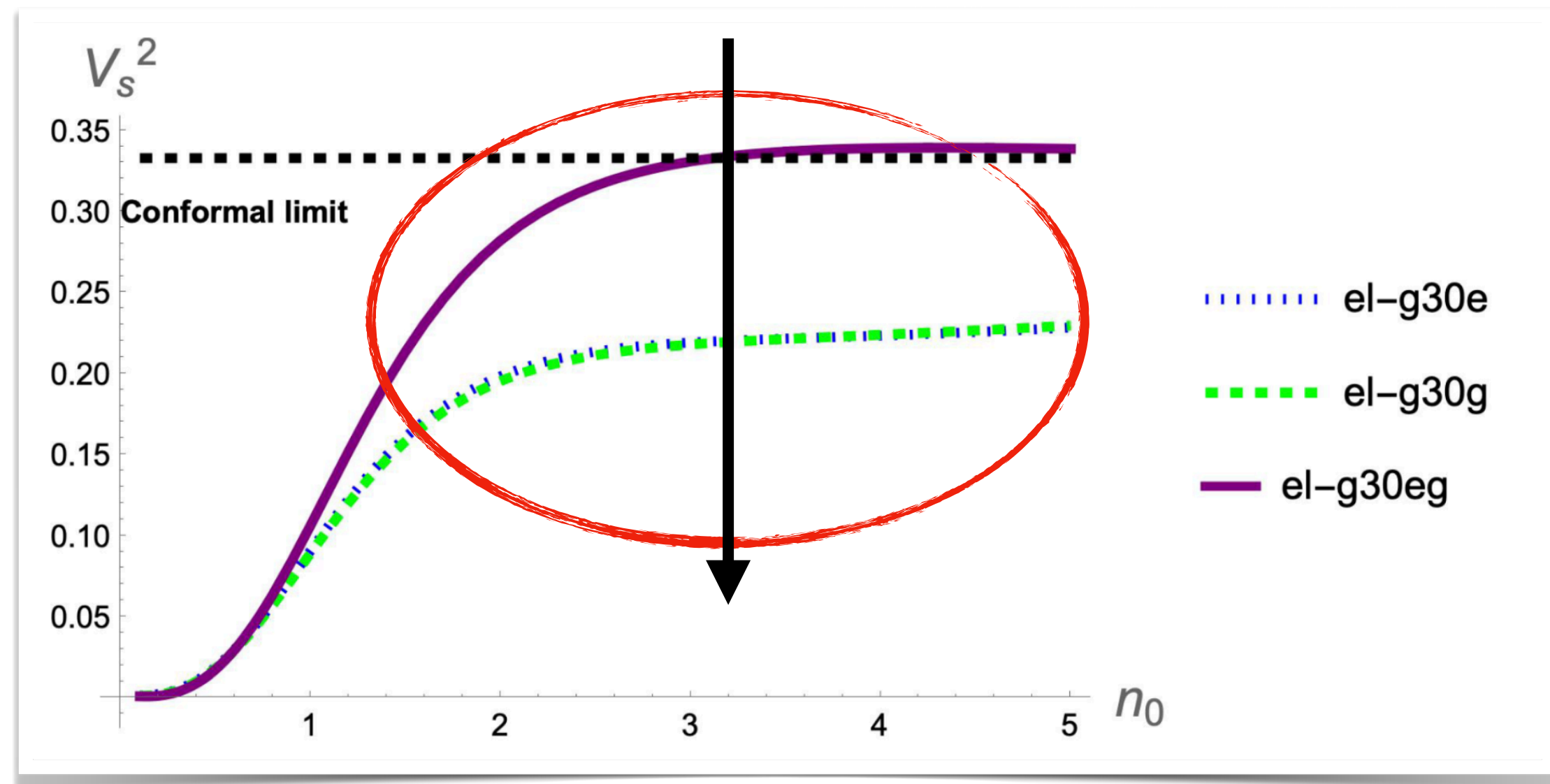
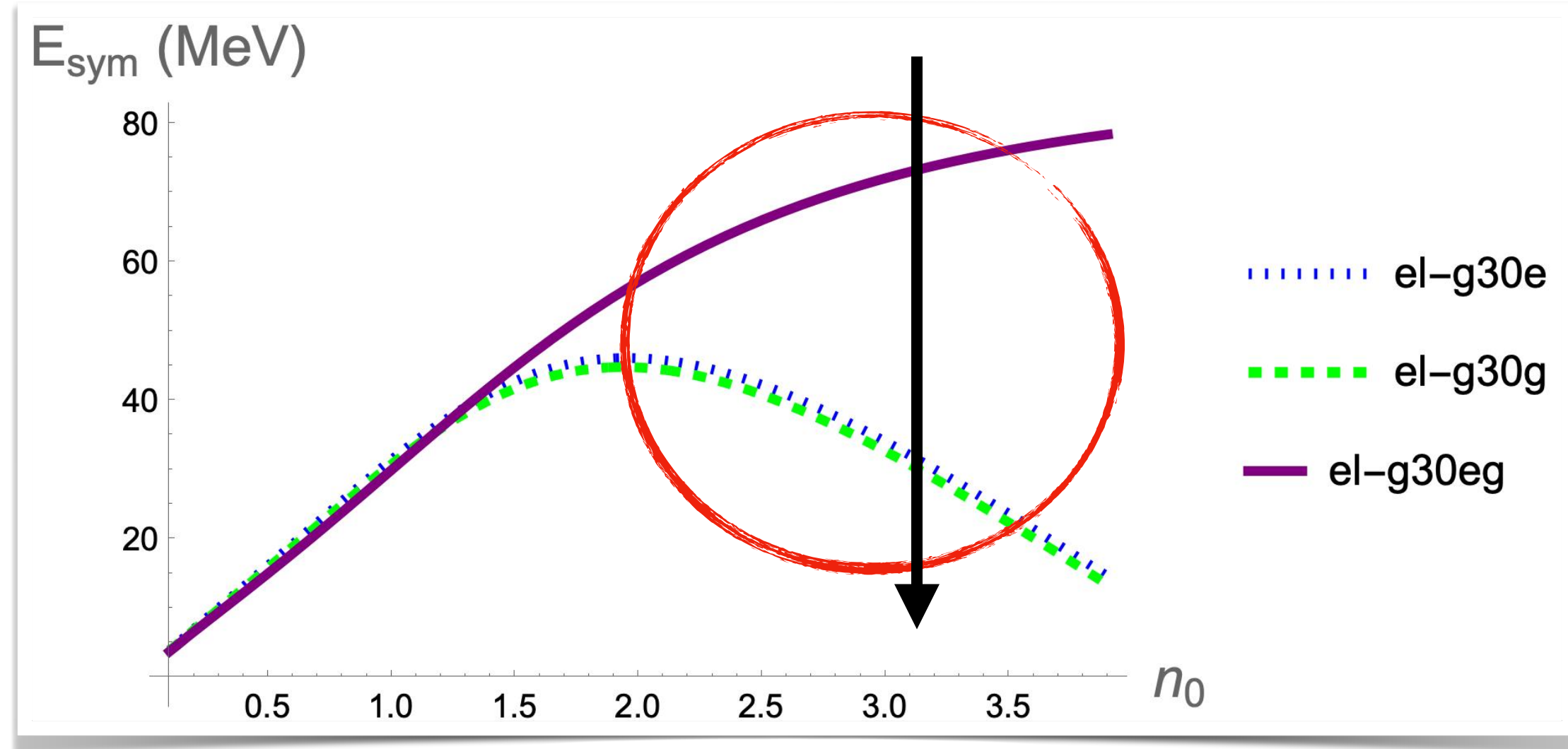
$\text{GW170817 } \Lambda_{1.4} \leq 580$

D. Adhikari et al., PREX, Phys. Rev. Lett. 126, 172502 (2021)
 B. T. Reed, F. J. Fattoyev, C. J. Horowitz, and J. Piekarewicz, Phys. Rev. Lett. 126, 172503 (2021)

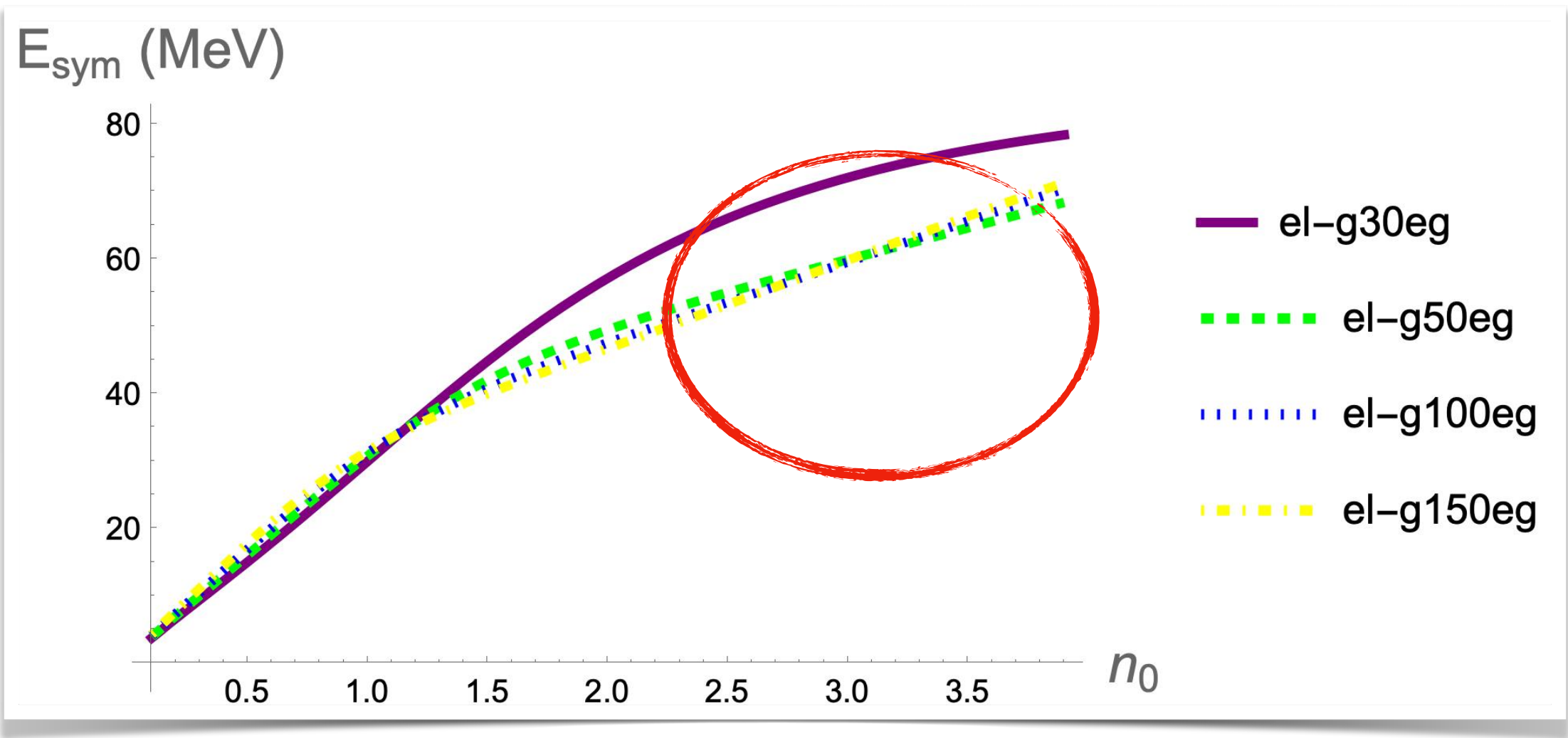
B. P. Abbott et al., LIGO Scientific, Virgo, Phys. Rev. Lett. 121, 161101 (2018)



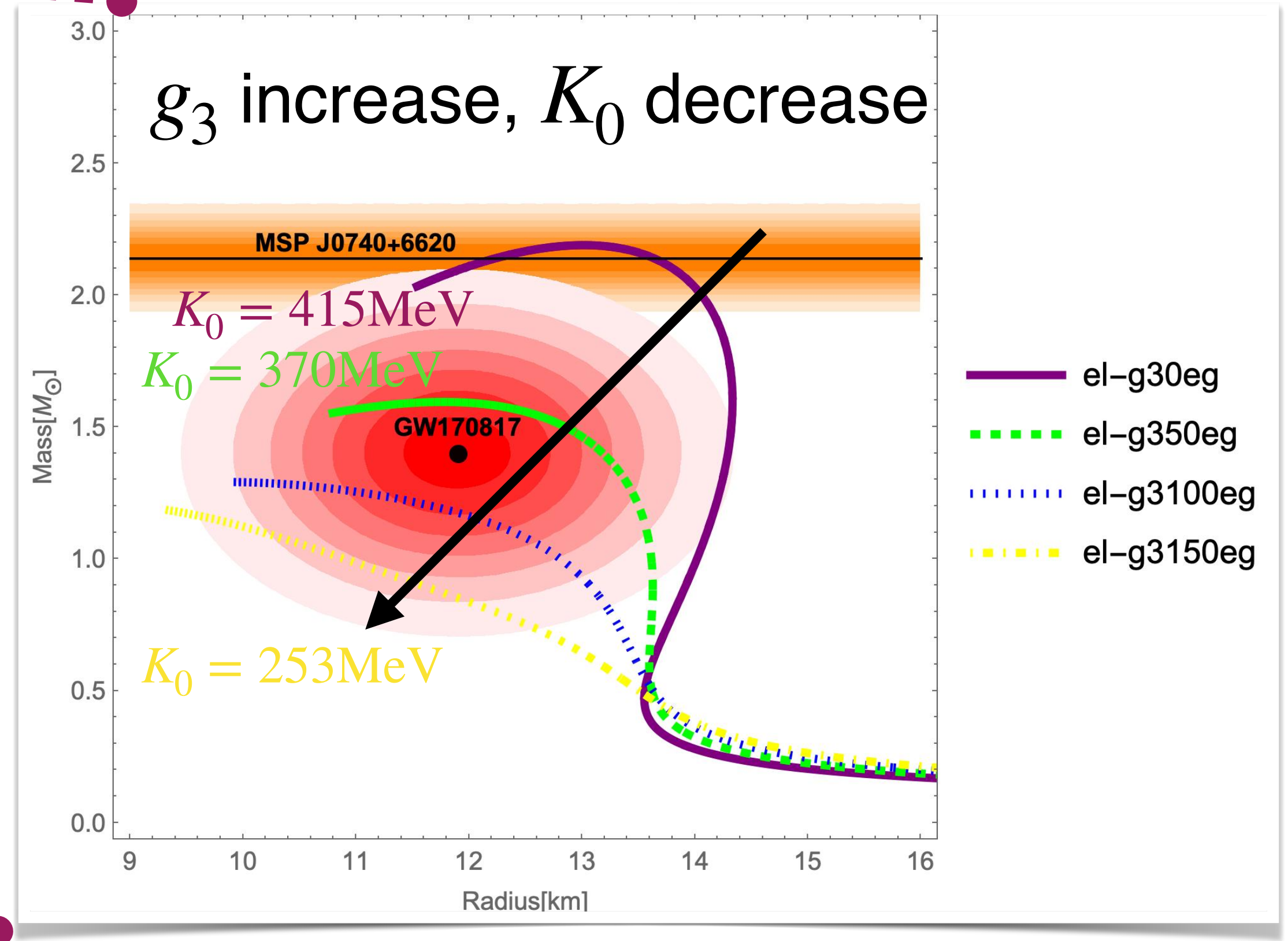
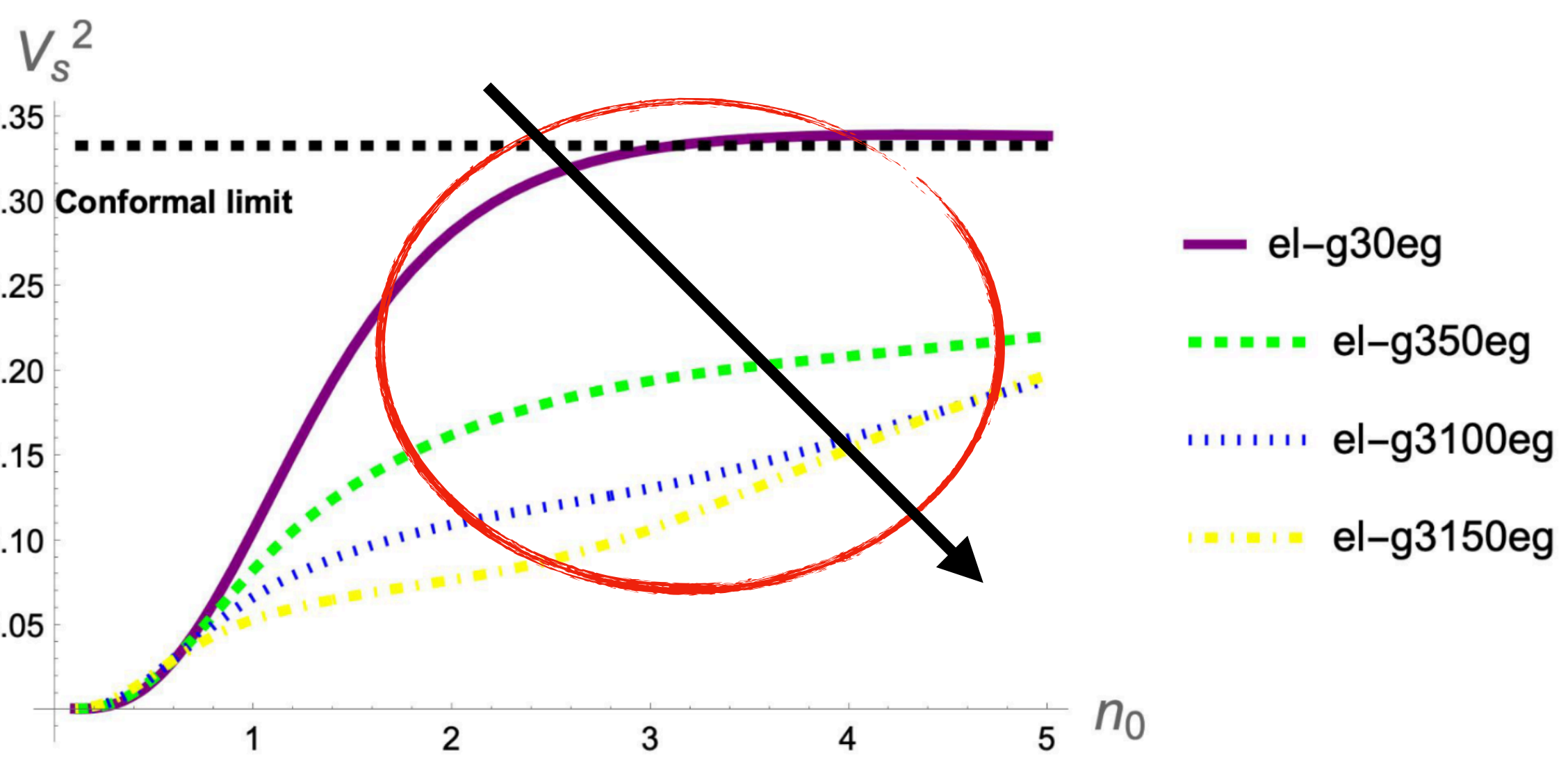
Comparison among different g_{aNN} cases



Comparison among different g_3 cases



H. T. Cromartie et al. (NANOGrav), Nature Astron. 4, 72 (2019).
 B. P. Abbott et al. (LIGO Scientific, Virgo), Phys. Rev. Lett. 121, 161101 (2018),



Quite different parameter space from EFT view



南京大學

MeV

	$C_{\sigma\delta^2}$	$C_{\sigma^2\delta^2}$
Zabari-19	± 1.77	± 0.004
FSU- $\delta 6.7$	—	2.63
el-g30g	-1860	-9.40
el-g30e	-1940	-9.71
el-g30eg	-1480	-7.70
el-g350eg	-1690	-8.75
el-g3100eg	-2190	-11.0
el-g3150eg	-2160	-11.0

	σ		δ	
	p_4	p_2	p_4	p_2
el-g30g	51.7%	48.3%	77.9%	22.1%
el-g30e	51.2%	48.7%	77.2%	22.8%
el-g30eg	54.2%	45.8%	81.5%	18.5%
el-g350eg	52.4%	47.6%	77.3%	20.7%
el-g3100eg	49.2%	50.8%	74.4%	25.6%
el-g3150eg	48.9%	51.1%	74.3%	25.7%

Quite different parameter space!

Slight difference of configurations
but large difference at macroscopic level

N. Zabari, S. Kubis, and W. Wójcik, Phys. Rev. C 99, 035209 (2019)
F. Li, B.-J. Cai, Y. Zhou, W.-Z. Jiang, and L.-W. Chen, Astrophys. J. 929, 183 (2022).

Strangeness in this framework under RMF (Neglecting the 4-quark configurations but with **explicit** symmetry breaking terms at leading order)



In collaboration with Lu-Qi Zhang (张璐琦)

$$\mathcal{V}_M = c_2 \text{Tr} S'^2 - c_4 \text{Tr} S'^4 - b_1 \text{Tr} (\xi S'^3) - 2G \text{Tr} (\xi S')$$

$$\begin{aligned} \mathcal{V}_V = & \tilde{h}_2 \text{Tr} (V^2 S'^2) + a_1 \epsilon^{ijk} \epsilon^{lmn} (V)_{il} (V)_{jm} (S'^2)_{kn} + b_2 \text{Tr} (V^2 \xi S') \\ & + b_3 \epsilon^{ijk} \epsilon^{lmn} (V)_{il} (V)_{jm} (\xi S')_{kn} + \tilde{g}_3 \text{Tr} V^4 + \tilde{a}_2 \epsilon^{ijk} \epsilon^{lmn} (V)_{il} (V)_{jm} (V^2)_{kn} \end{aligned}$$

$$\mathcal{L}_{\text{RMF}}^B = \text{Tr} (\bar{B} i \gamma_\mu \partial^\mu B) + c \text{Tr} [\bar{B} \gamma_0 V B] + c' \text{Tr} [\bar{B} \gamma_0 B V]$$

$$+ h \epsilon^{ijk} \epsilon^{lmn} (\bar{B})_{il} (V \gamma_0)_{jm} (B)_{kn} - g \text{Tr} [\bar{B} S' B]$$

$$- e \epsilon^{ijk} \epsilon^{lmn} (\bar{B})_{il} (S')_{jm} (B)_{kn} - b_4 \text{Tr} [\bar{B} \xi B] - b_5 \epsilon^{ijk} \epsilon^{lmn} (\bar{B})_{il} (\xi)_{jm} (B)_{kn}$$

Mass splittings (beta equilibrium)

Strangeness in this framework under RMF (Neglecting the 4-quark configurations)

arXiv:2512.23477 [nucl-th], (2025), YM, Y. L. Ma and L.-Q. Zhang



$$S = \frac{1}{\sqrt{2}} (\lambda_8 f_0 + \lambda_3 a_0) + \frac{1}{\sqrt{3}} \mathbf{I} \cdot \boldsymbol{\sigma}$$

$$V = \frac{1}{2} \begin{pmatrix} \rho + \omega & 0 & 0 \\ 0 & -\rho + \omega & 0 \\ 0 & 0 & \sqrt{2}\phi \end{pmatrix}$$

$$B = \begin{pmatrix} \frac{\Lambda}{\sqrt{6}} + \frac{\Sigma^0}{\sqrt{2}} & & & \\ & \Sigma^- & & \\ & & \Sigma^+ & \\ & & & \frac{\Lambda}{\sqrt{6}} - \frac{\Sigma^0}{\sqrt{2}} \\ & & & & \Xi^- & \\ & & & & & \Xi^0 \\ & & & & & & -\frac{2\Lambda}{\sqrt{6}} \end{pmatrix} \begin{matrix} p \\ n \\ \\ \\ \\ \end{matrix}$$

Neglected in EOS after the determination of mass spectrum

Physical couplings and mass formula



$$g_{\rho NN} = -\frac{1}{2}(c + h)$$

$$g_{\omega NN} = -\frac{1}{2}(c - h)$$

$$g_{\omega\Lambda\Lambda} = -\frac{1}{6}(c + c' - 4h)$$

$$g_{\sigma NN} = g_{\sigma\Lambda\Lambda} = -\frac{1}{\sqrt{3}}(g - e)$$

$$\xi = \xi_1\lambda_1 + \xi_3\lambda_3 + \xi_8\lambda_8$$

Non-zero $\langle a_0 \rangle$ and $\langle f_0 \rangle$

Gell-Mann Okubo Formula

$$m_{\Sigma^+} = \frac{1}{2}(-2m_n + 3m_\Lambda - 2m_{\Xi^-} + 3m_{\Sigma^0})$$

$$m_{\Sigma^-} = \frac{1}{2}(2m_n - 3m_\Lambda + 2m_{\Xi^-} + m_{\Sigma^0})$$

$$m_{\Xi^0} = -m_n - m_p + 3m_\Lambda - m_{\Xi^-} + m_{\Sigma^0}.$$

$$m_{a_0}^2 + m_{f_0}^2 = 2m_\sigma^2$$

Hadron spectra and nuclear matter properties

	Empirical	$\sigma_{\pi N-75^+}$	$\sigma_{\pi N-100^-}$	$\sigma_{\pi N-400^-}$	$\sigma_{\pi N-600^-}$
$n_0(\text{fm}^{-3})$	0.1550 ± 0.0500	0.1592	0.1592	0.1592	0.1592
$e_0(\text{MeV})$	-15.00 ± 1.00	-16.00	-16.00	-16.02	-16.00
$K(n_0)(\text{MeV})$	230.0 ± 30.0	240.8	241.3	241.6	239.2
$E_{\text{sym}}(n_0)(\text{MeV})$	30.90 ± 1.90	30.00	30.00	30.01	30.00
$L(n_0)(\text{MeV})$	52.50 ± 17.50	54.91	52.18	70.94	76.74

→ Align with the empirical values

$$U_\Lambda \approx -28 \text{ MeV}$$

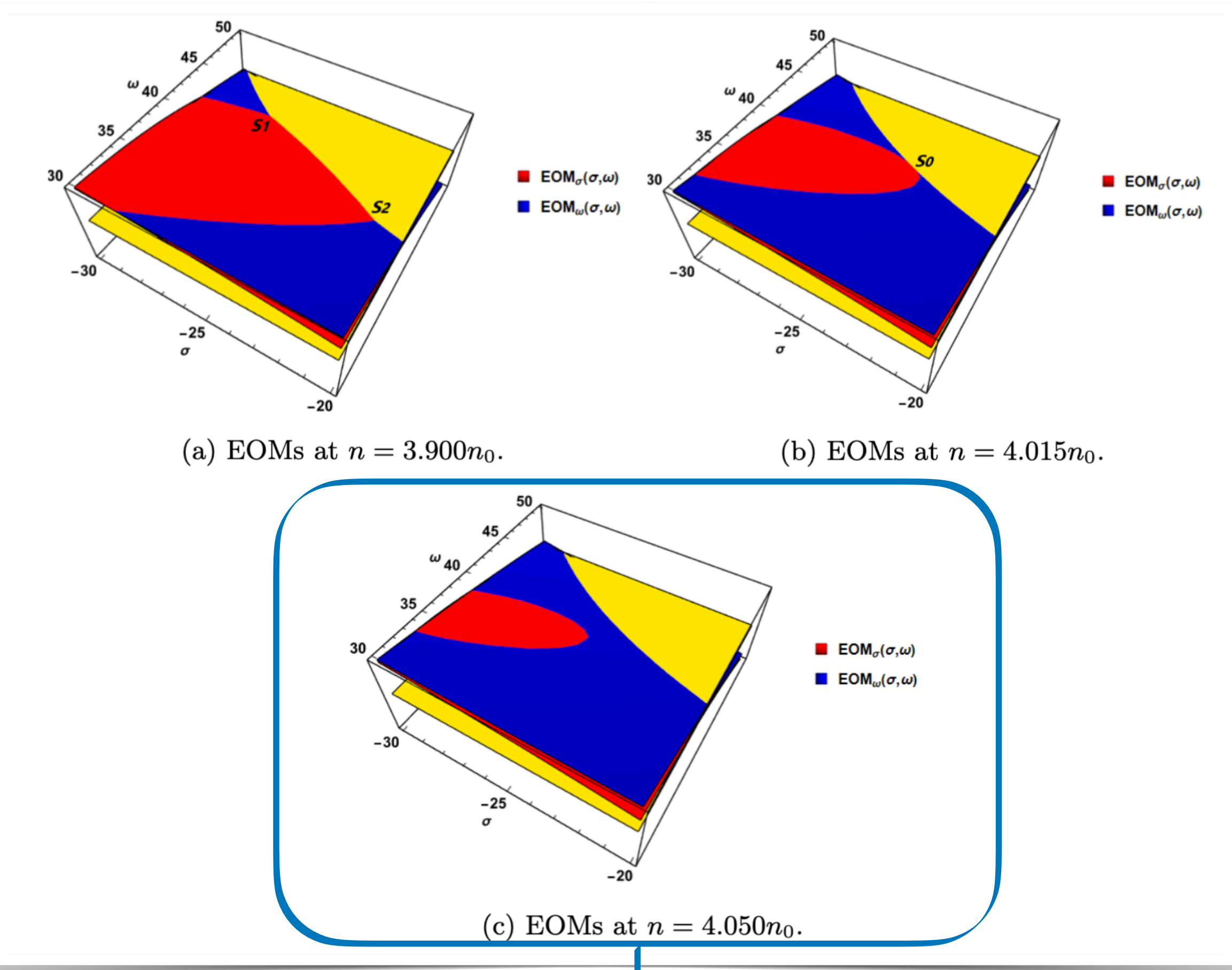
$$m_N = m + \sigma_{\pi N}(0)$$

Account for the contribution of spontaneous and explicit breaking

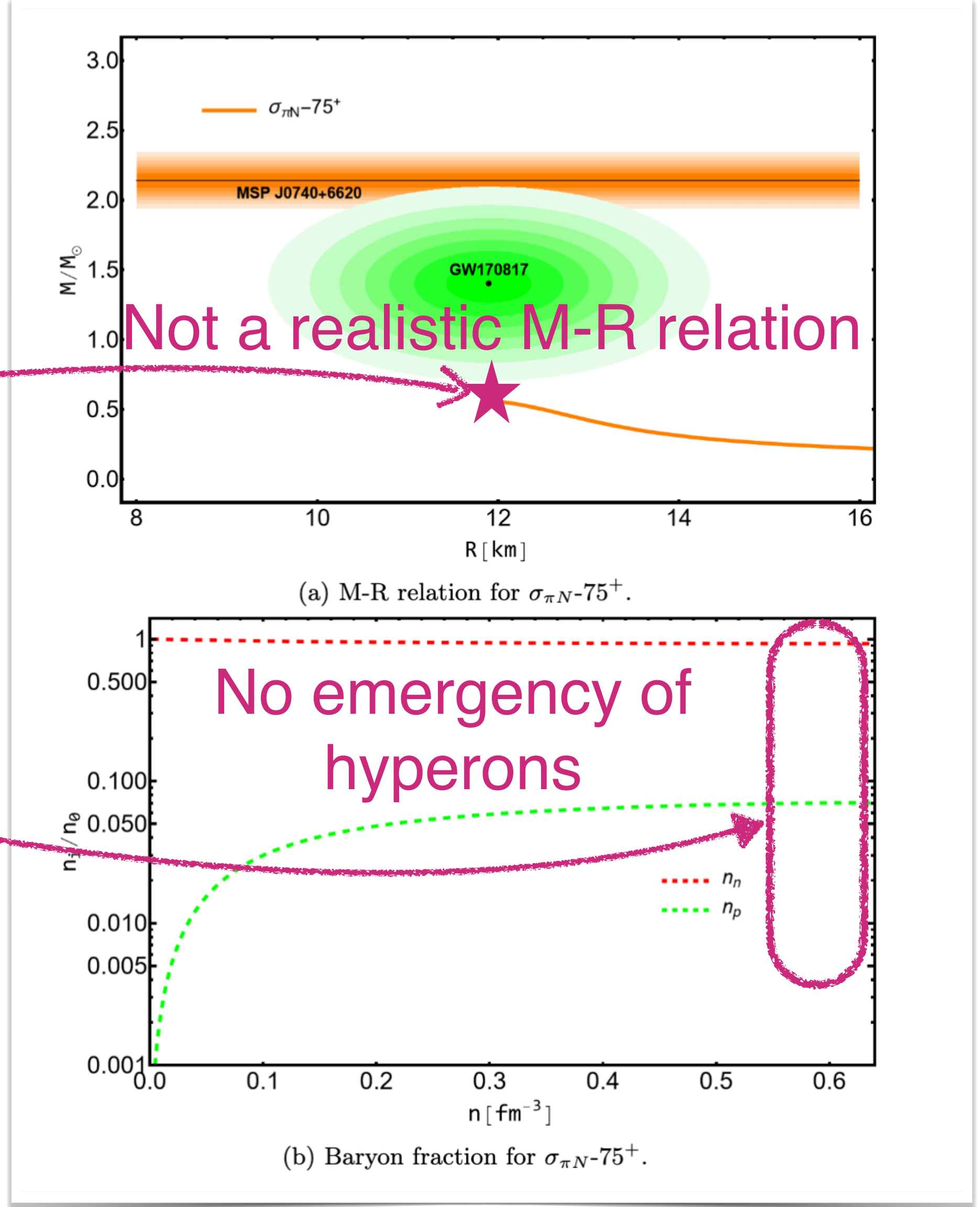
	Empirical	$\sigma_{\pi N-75^+}$	$\sigma_{\pi N-100^-}$	$\sigma_{\pi N-400^-}$	$\sigma_{\pi N-600^-}$
m_n	$939.565 \pm (5 \times 10^{-7})$	939.565	939.565	939.565	939.565
m_p	$938.272 \pm (2.9 \times 10^{-7})$	938.272	938.272	938.272	938.272
m_Λ	$1115.68 \pm (0.006)$	1115.59	1115.54	1115.57	1115.58
m_{Σ^+}	1189.37 ± 0.06	1192.30	1191.21	1191.74	1191.79
m_{Σ^0}	1192.64 ± 0.02	1192.17	1192.18	1192.84	1191.98
m_{Σ^-}	1197.45 ± 0.03	1192.03	1191.15	1191.95	1192.16
m_{Ξ^0}	1314.82 ± 0.21	1331.34	1330.65	1330.90	1330.90
m_{Ξ^-}	1321.70 ± 0.09	1329.77	1329.30	1329.82	1329.98
m_{a_0}	995.000 ± 25.000	980.132	979.998	980.024	980.040
m_{f_0}	995.000 ± 15.000	990.119	989.962	989.971	989.974
m_σ	475.000 ± 75.000	985.183	984.993	986.010	985.019
m_ρ	773.000 ± 2.000	775.261	775.260	775.260	775.260
m_ω	782.660 ± 0.13	782.659	782.660	782.660	782.660
m_ϕ	1019.46 ± 0.02	1019.46	1019.46	1019.46	1019.46
$\sigma_{\pi N}(0)$	60.5000 ± 28.5000	75.0541	-104.048	-402.087	-625.663
m	878.419 ± 29.1465	863.946	1043.05	1341.09	1564.66

Problems in M-R relation and RMF approach for $\sigma_{\pi N-75}^+$

Solution plane for EOMs of mesons



No continuous solutions

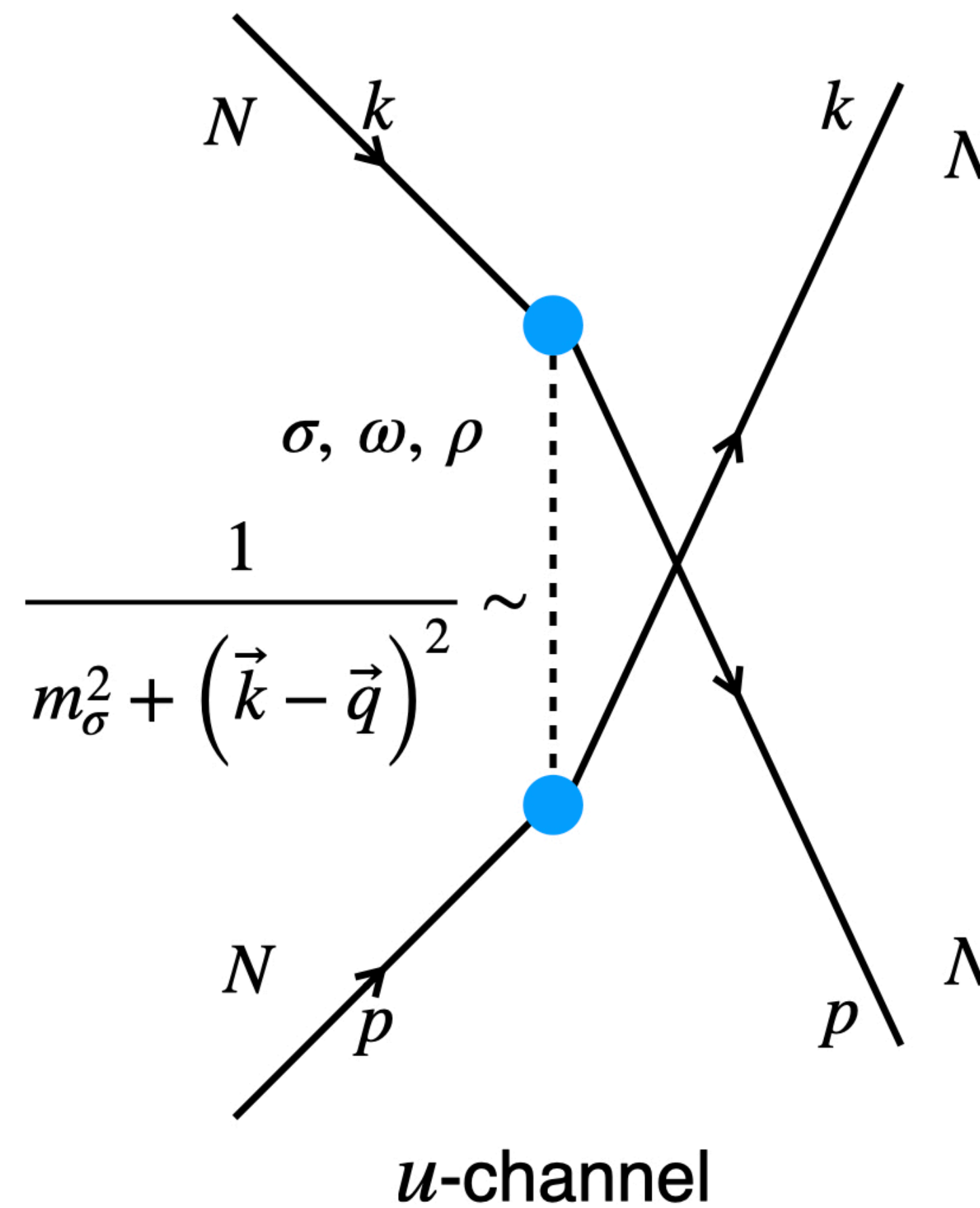
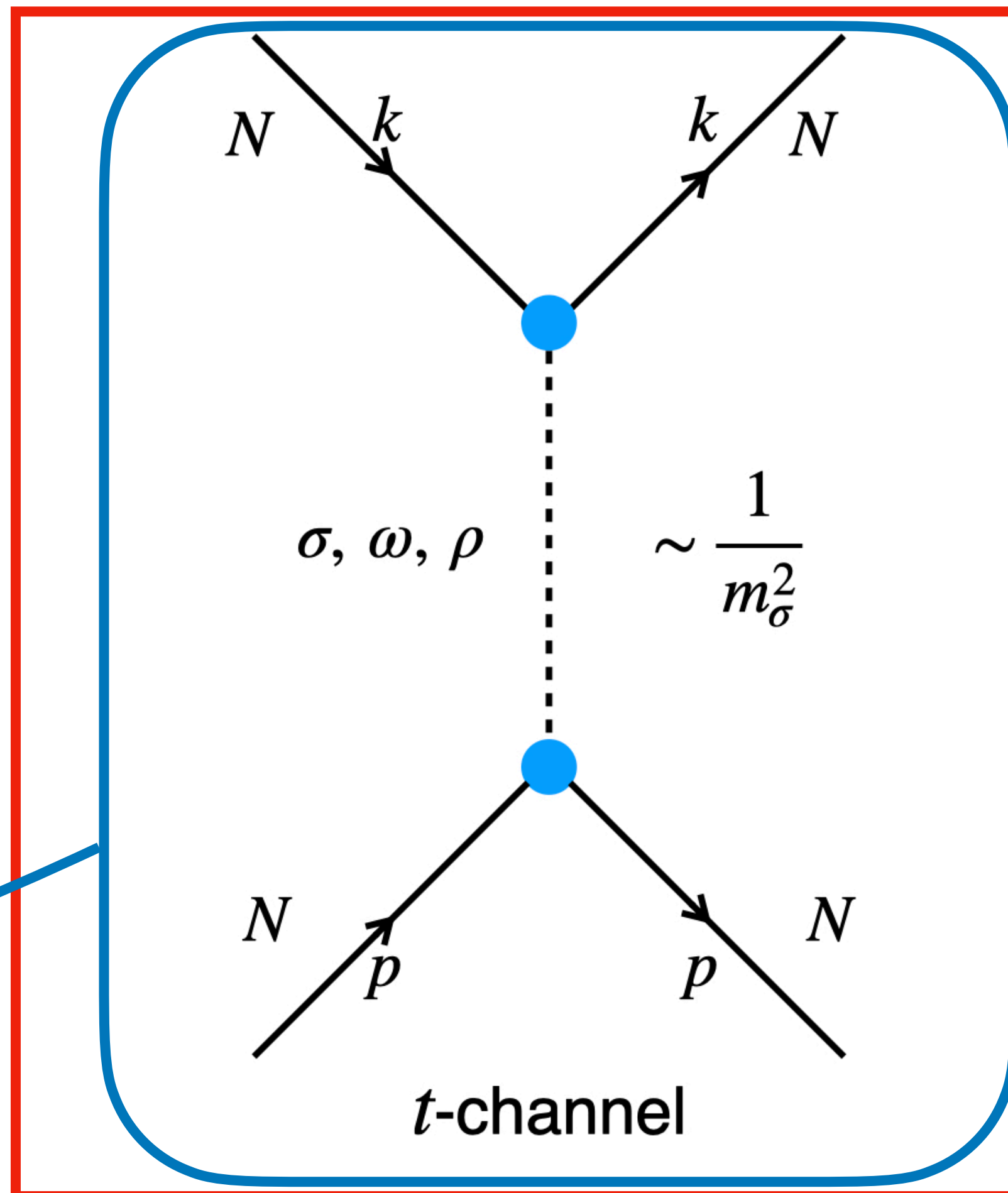


Not a realistic M-R relation

No emergency of hyperons

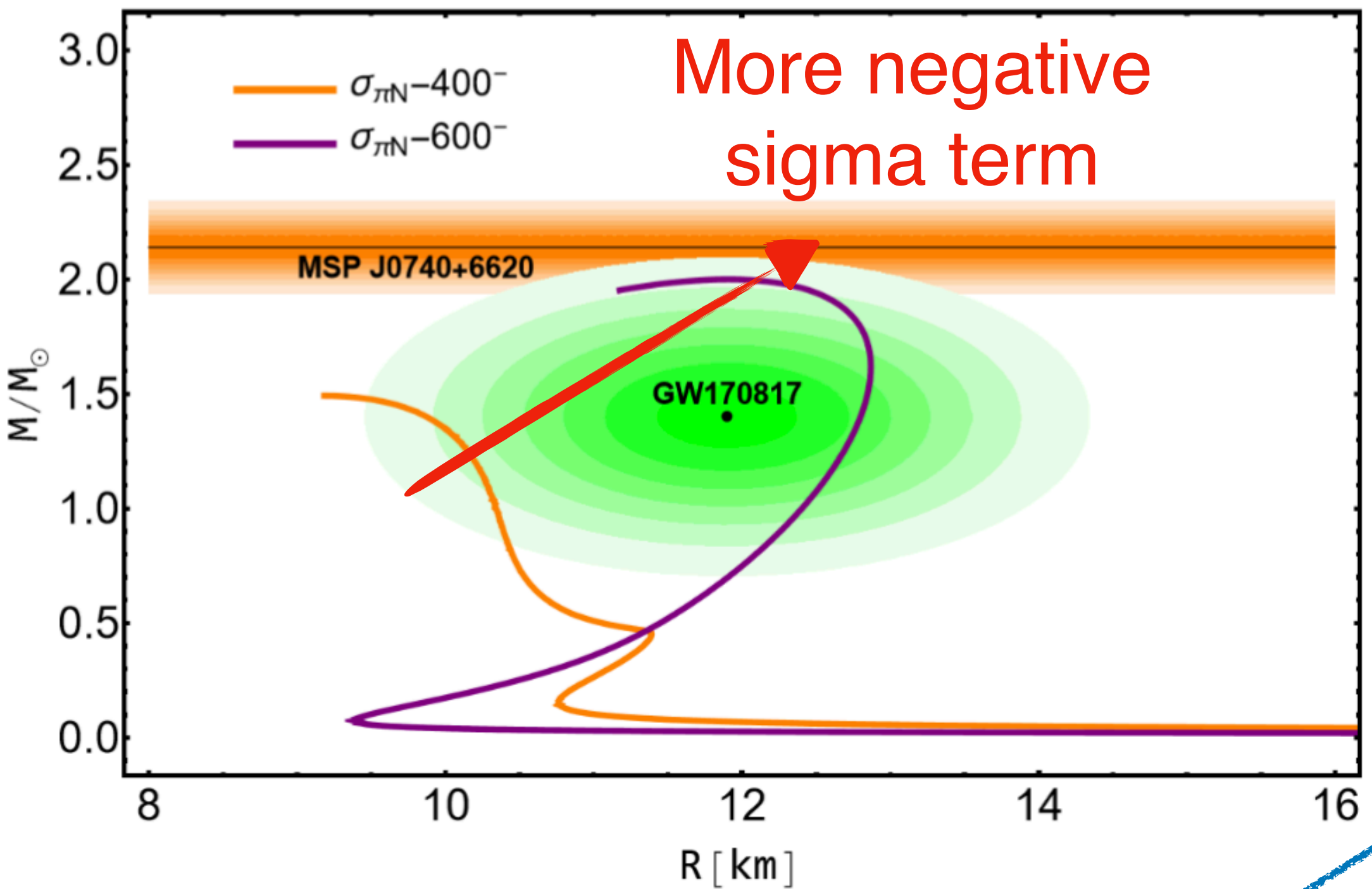
Ignorance of exchange terms of nucleon interaction

Relativistic mean field



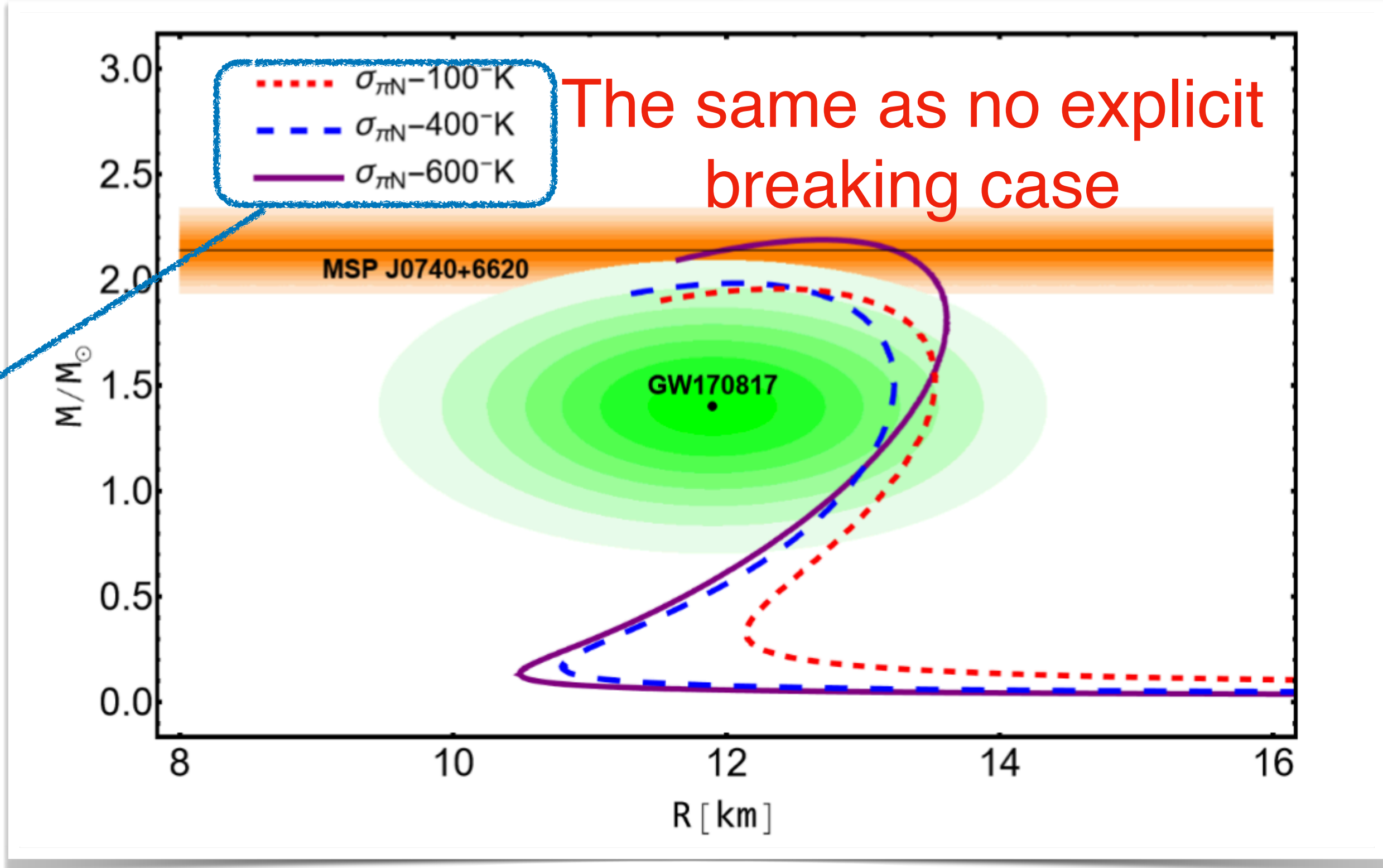
Relativistic Hartree-Fock

Effects of sigma term and incompressibility



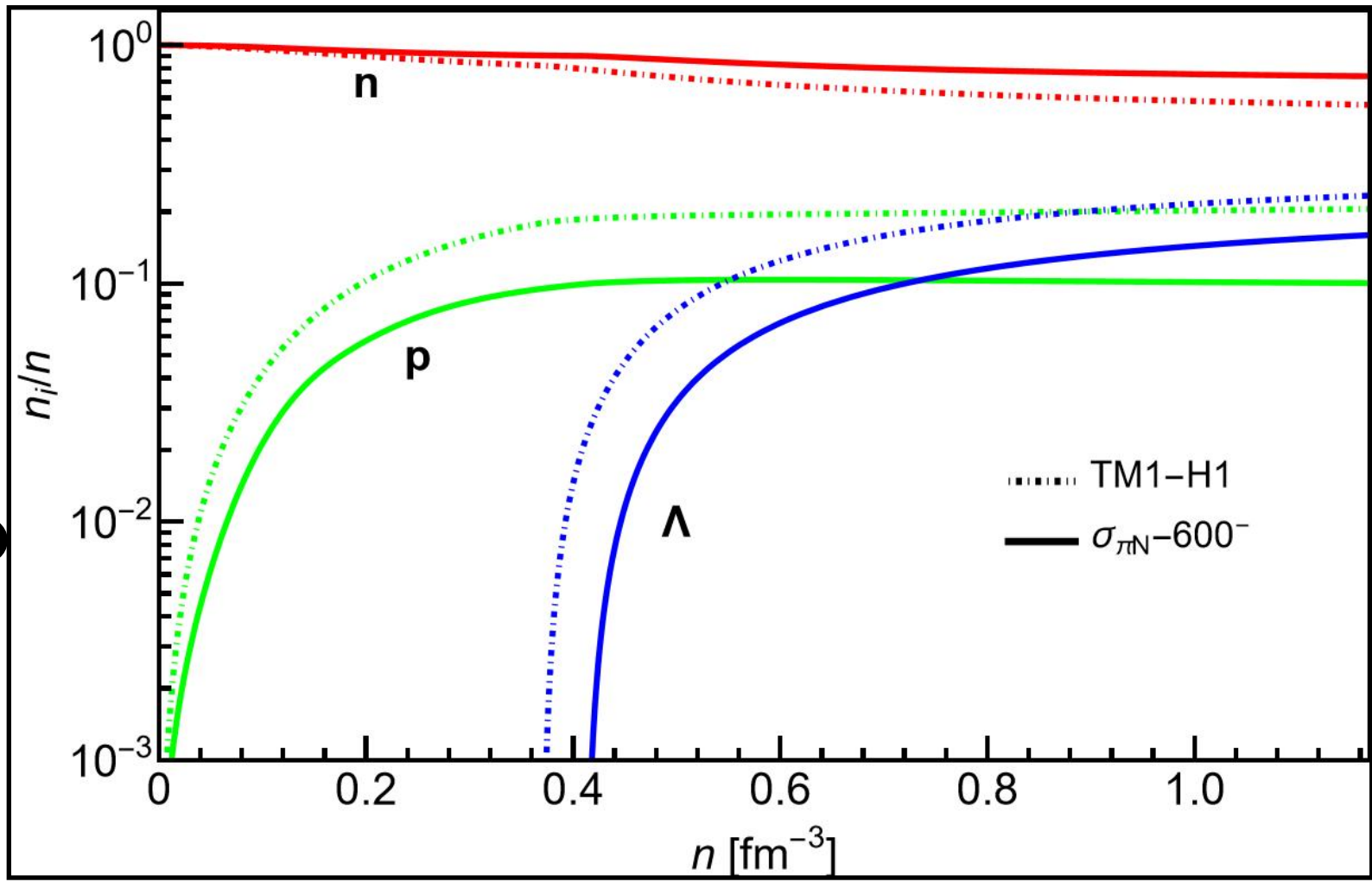
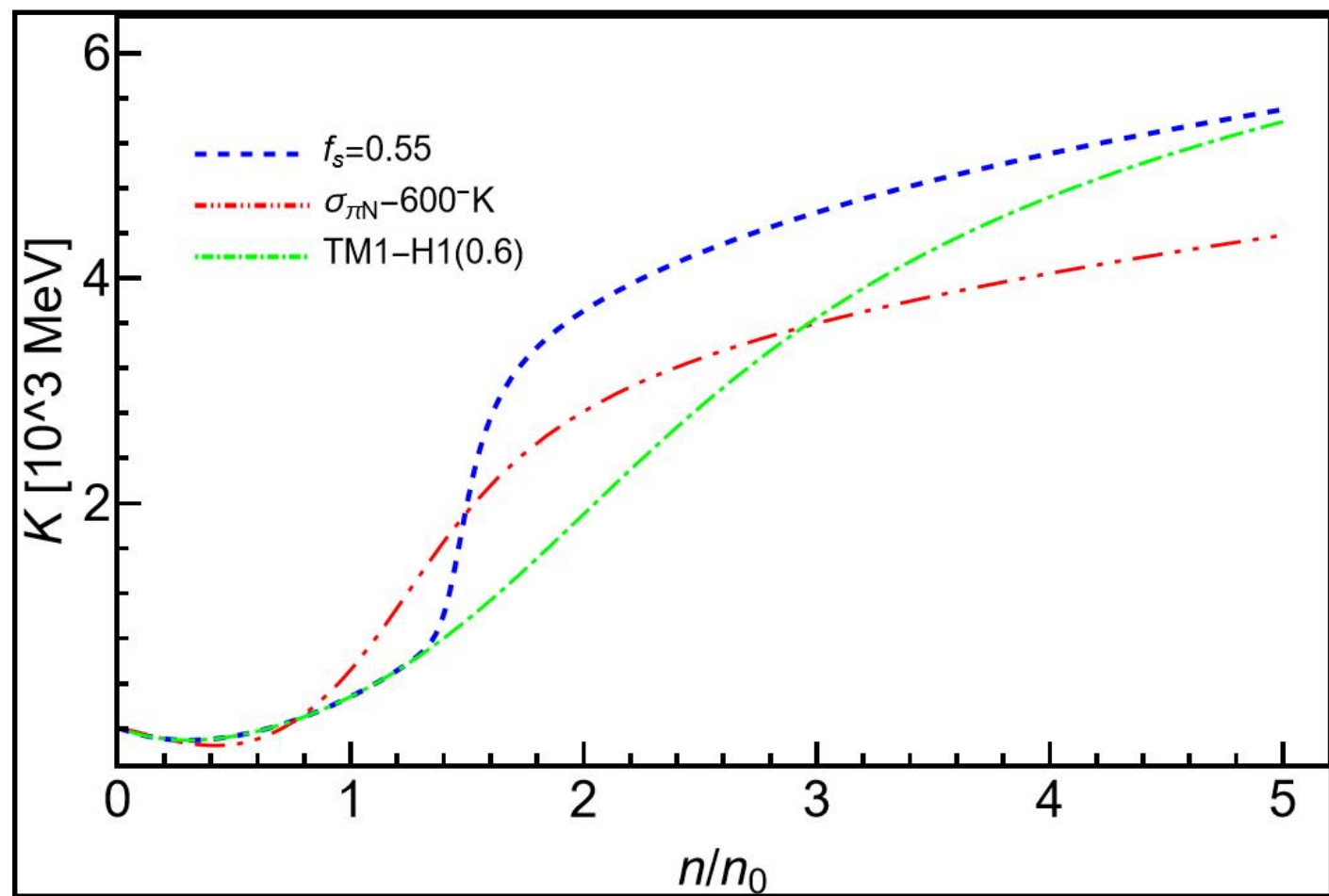
Still negative sigma term

	Empirical	$\sigma_{\pi N} = -100$ MeV	$\sigma_{\pi N} = -400$ MeV	$\sigma_{\pi N} = -600$ MeV
n_0 (fm ⁻³)	0.1550 ± 0.0500	0.1592	0.1592	0.1592
e_0 (MeV)	-15.00 ± 1.00	-16.00	-15.99	-16.00
$K(n_0)$ (MeV)	—	521.9	520.3	518.8
$E_{\text{sym}}(n_0)$ (MeV)	30.90 ± 1.90	30.00	30.00	30.01
$L(n_0)$ (MeV)	52.50 ± 17.50	80.15	93.28	76.64

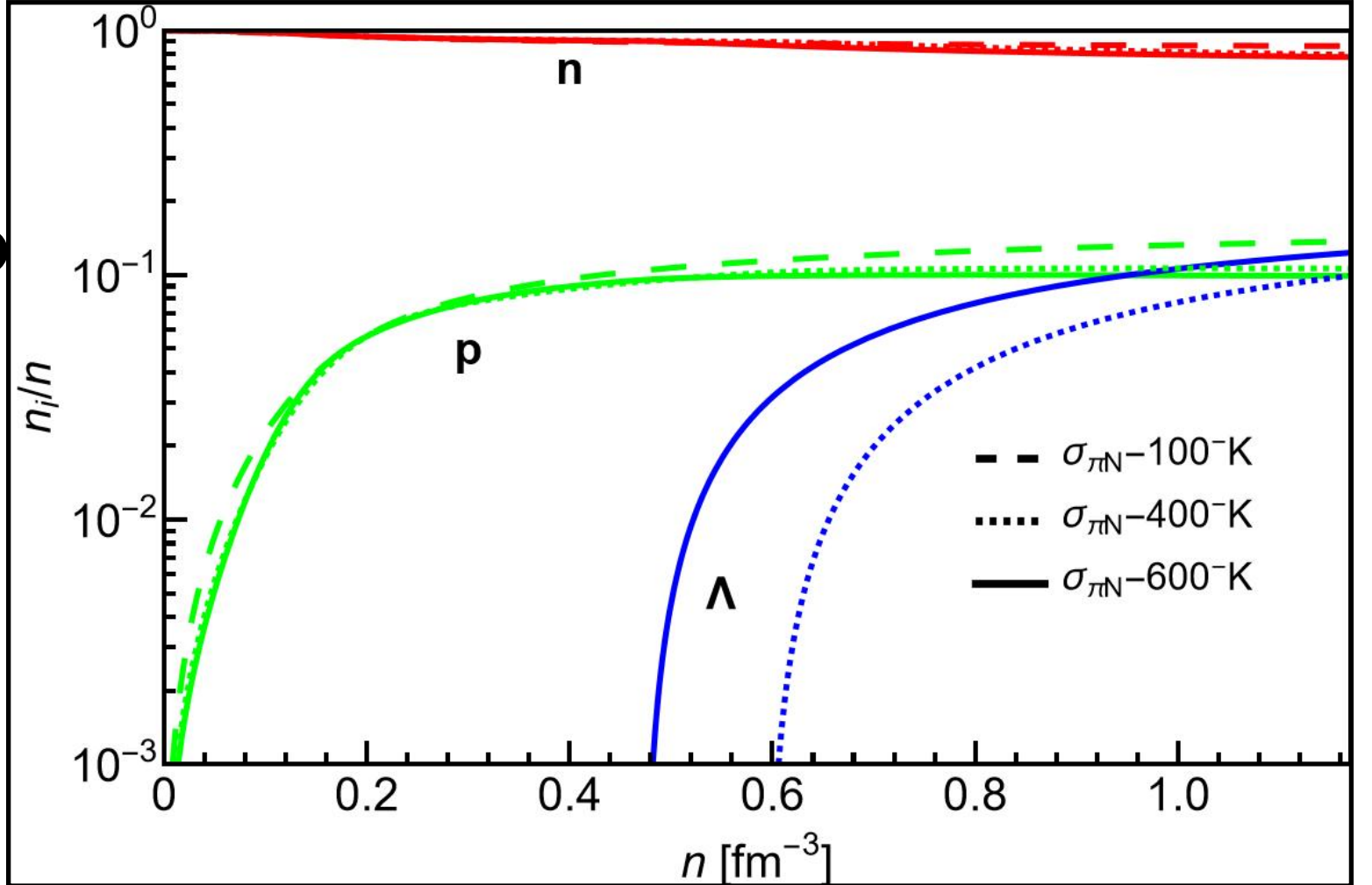
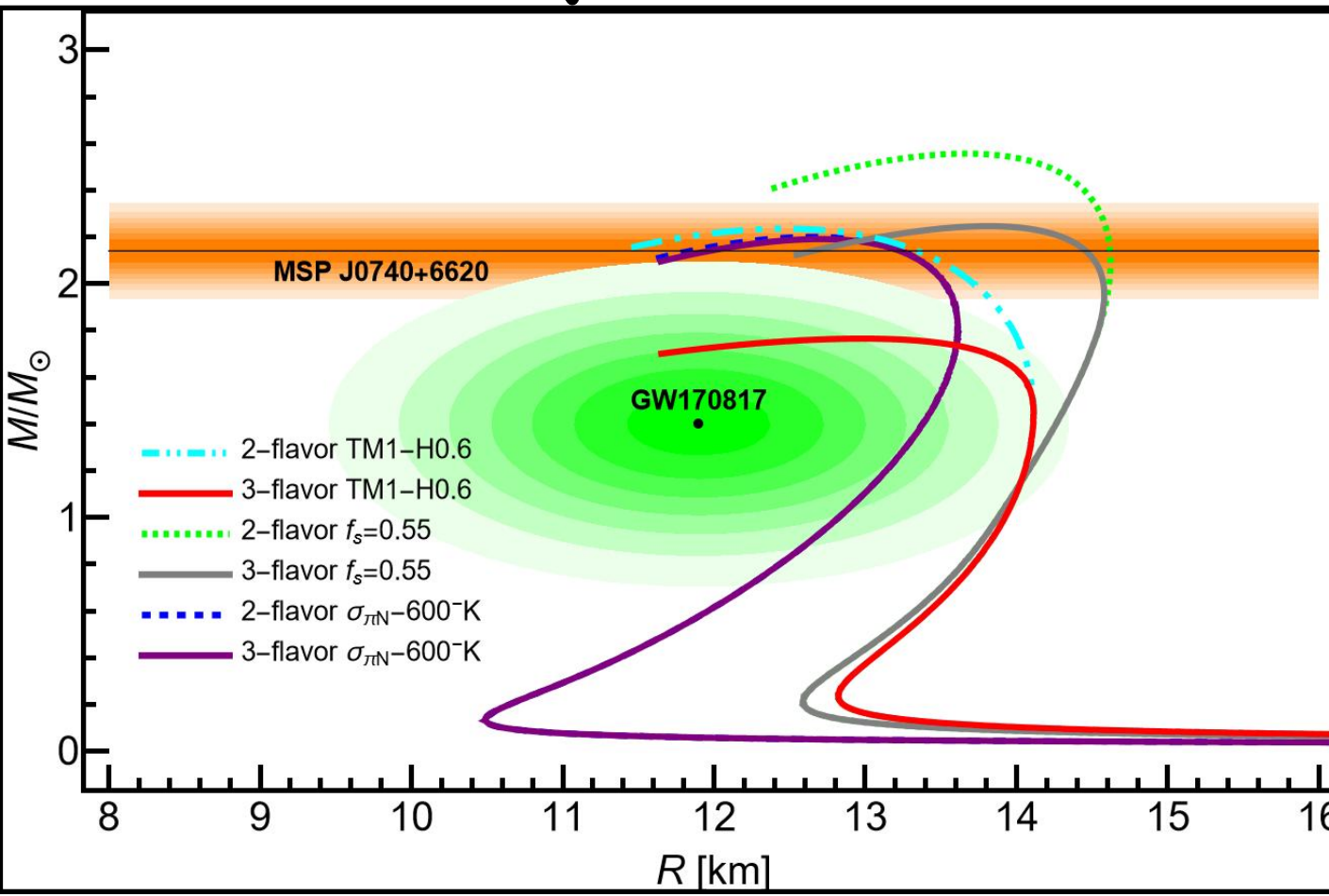


Comparison with Walecka models

Y. Zhang, J. Hu, and P. Liu, Phys. Rev. C 97, 015805 (2018).
 K. A. Maslov, E. E. Kolomeitsev, and D. N. Voskresensky, Phys. Rev. C 92, 052801 (2015).



Hyperon Ratio



What could be learned?

- I. The low energy EFTs/models of QCD can reproduce the **vacuum spectra**, NM properties and NS structures with **appropriate parameter choice but different from past studies based on Walecka models**;
- II. A **scaling scheme** for parameters to cover different physical regions may be crucial to connect the QCD symmetry patterns and NS observations;
- III. At high densities, Fock terms (**quantum exchange effects**) ignored in RMF may play an important role.



Thank you!

Backup



Outline

嚴謹求實
勤奮創新

- Motivation (How to connect the **microscopic symmetries** to the rich **macroscopic phenomena**)
- Theoretical framework and phenomenological analysis (**Nuclear matter** properties and **neutron star** structures with an extended linear sigma model (**chiral symmetry**))

The lowest order Lagrangians (The system only with nucleons)



The scalar meson masses by spontaneous chiral symmetry breaking

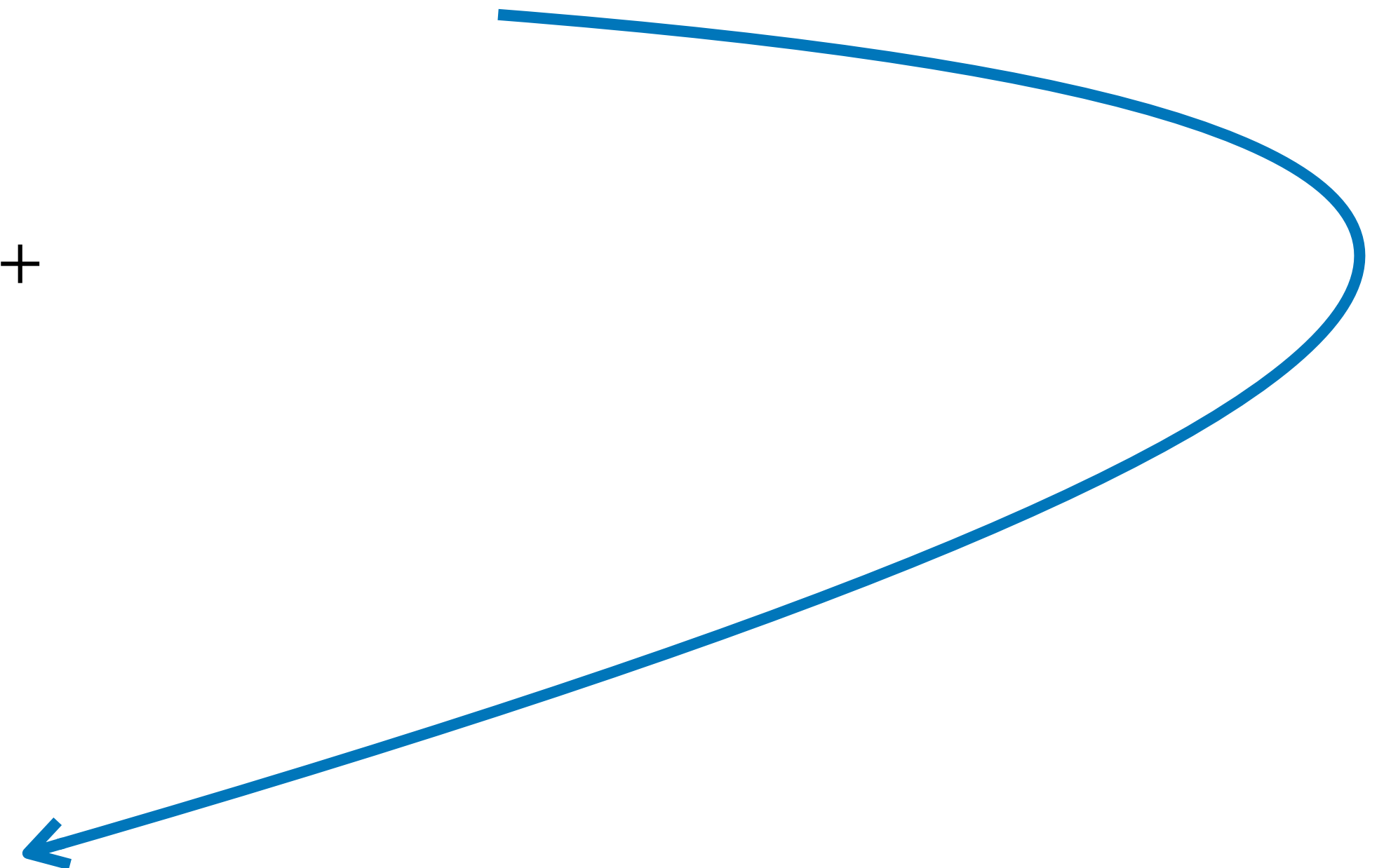
$$\mathcal{L}_M = \frac{1}{2} \text{Tr} \left(\partial_\mu \Phi' \partial^\mu \Phi'^\dagger \right) + \frac{1}{2} \text{Tr} \left(\partial_\mu \hat{\Phi}' \partial^\mu \hat{\Phi}'^\dagger \right) + c_2 \text{Tr} \left(\Phi' \Phi'^\dagger \right) - c_4 \text{Tr} \left(\Phi' \Phi'^\dagger \Phi' \Phi'^\dagger \right) - d_2 \text{Tr} \left(\hat{\Phi}' \hat{\Phi}'^\dagger \right) - e_3 \left(\epsilon_{abc} \epsilon^{def} \Phi'_d{}^a \Phi'_e{}^b \hat{\Phi}'_f{}^c + \text{h.c.} \right) - c_3 \left[\gamma_1 \ln \left(\frac{\det \Phi'}{\det \hat{\Phi}'^\dagger} \right) + (1 - \gamma_1) \ln \left(\frac{\text{Tr} \left(\Phi' \hat{\Phi}'^\dagger \right)}{\text{Tr} \left(\hat{\Phi}' \Phi'^\dagger \right)} \right) \right]^2$$

Two quark configurations mixing

- A. H. Fariborz, R. Jora, and J. Schechter, Phys. Rev. D 72, 034001 (2005)
- A. H. Fariborz, R. Jora, and J. Schechter, Phys. Rev. D 77, 034006 (2008)
- A. H. Fariborz, R. Jora, and J. Schechter, Phys. Rev. D 79, 074014 (2009)



$$\begin{aligned}
\mathcal{L}_V = & -\frac{1}{8} \text{Tr} \left(L_{\mu\nu} L^{\mu\nu} + R_{\mu\nu} R^{\mu\nu} \right) + g_1 \left[\text{Tr} \left(\partial_\nu R_\mu R^\mu R^\nu \right) + \text{Tr} \left(\partial_\nu L_\mu L^\mu L^\nu \right) \right] + \\
& g_2 \left[\text{Tr} \left(\partial_\nu R_\mu R^\nu R^\mu \right) + \text{Tr} \left(\partial_\nu L_\mu L^\nu L^\mu \right) \right] + g_3 \left[\text{Tr} \left(R_\mu R^\mu R_\nu R^\nu \right) + \text{Tr} \left(L_\mu L^\mu L_\nu L^\nu \right) \right] + \\
& g_4 \left[\text{Tr} \left(R_\mu R^\nu R_\mu R^\nu \right) + \text{Tr} \left(L_\mu L^\nu L_\mu L^\nu \right) \right] + h_1 \left[\text{Tr} \left(\Phi'^\dagger \Phi' R_\mu R^\mu \right) + \text{Tr} \left(\Phi' \Phi'^\dagger L_\mu L^\mu \right) \right] + \\
& h_2 \left[\text{Tr} \left(L^\mu \Phi' R_\mu \Phi'^\dagger \right) \right] + h_3 \left[\text{Tr} \left(\Phi'^\dagger \partial_\mu \Phi' R^\mu \right) + \text{Tr} \left(\Phi' \partial_\mu \Phi'^\dagger L^\mu \right) \right] + \\
& \frac{a_1}{2} \epsilon_{abc} \epsilon^{def} \left[\left(R_\mu \right)_{ad} \left(R_\nu \right)_{be} \left(\Phi'^\dagger \Phi \right)_{cf} + \left(L_\mu \right)_{ad} \left(L_\nu \right)_{be} \left(\Phi \Phi'^\dagger \right)_{cf} \right] + \\
& \frac{a_2}{2} \epsilon_{abc} \epsilon^{def} \left[\left(R_\mu \right)_{ad} \left(R_\nu \right)_{be} \left(R^\mu R^\nu \right)_{cf} + \left(L_\mu \right)_{ad} \left(L_\nu \right)_{be} \left(L^\mu L^\nu \right)_{cf} \right] + \\
& \frac{a_3}{2} \epsilon_{abc} \epsilon^{def} \left[\left(R_\mu \right)_{ad} \left(R^\mu \right)_{be} \left(R^\nu R_\nu \right)_{cf} + \left(L_\mu \right)_{ad} \left(L^\mu \right)_{be} \left(L^\nu L_\nu \right)_{cf} \right] + \\
& \frac{a_4}{2} \epsilon_{abc} \epsilon^{def} \left[\left(R_\mu \right)_{ad} \left(R^\nu \right)_{be} \left(\partial^\mu R_\nu \right)_{cf} + \left(L_\mu \right)_{ad} \left(L^\nu \right)_{be} \left(\partial^\mu L_\nu \right)_{cf} \right]
\end{aligned}$$



The vector meson masses by spontaneous chiral symmetry breaking

Di-quark approximation

L. Olbrich, Master's thesis, Goethe U., Frankfurt (main) (2015).

L. Olbrich, M. Zétényi, F. Giacosa, and D. H. Rischke, Phys. Rev. D 93, 034021 (2016).

$$N_{R, L}^{(RR)} = \frac{1}{\sqrt{2}} \frac{1 \pm \gamma_5}{2} B, \quad N_{R, L}^{(LL)} = -\frac{1}{\sqrt{2}} \frac{1 \pm \gamma_5}{2} B$$



$$\begin{aligned} \mathcal{L}_B = & \text{Tr}(\bar{B} i \not{\partial} B) + c \text{Tr} \left(\bar{B} \gamma_\mu V^\mu B + \bar{B} \gamma_\mu \gamma_5 A^\mu B \right) + c' \text{Tr} \left(\bar{B} \gamma_\mu \bar{B} V^\mu + \bar{B} \gamma_\mu \gamma_5 \bar{B} A^\mu \right) + \\ & h \epsilon_{abc} \epsilon^{def} \left[(\bar{B})_{ad} \gamma_\mu (B)_{be} (V^\mu)_{cf} + (\bar{B})_{ad} \gamma_\mu \gamma_5 (B)_{be} (A^\mu)_{cf} \right] - \\ & \frac{g}{2} \text{Tr} \left[\bar{B} (\Phi' + \Phi'^\dagger) B + \bar{B} \gamma_5 (\Phi' - \Phi'^\dagger) B \right] - \\ & \frac{e}{2} \epsilon_{abc} \epsilon^{def} \left[(\bar{B})_{ad} (\Phi' + \Phi'^\dagger)_{be} (B)_{cf} + (\bar{B})_{ad} \gamma_5 (\Phi' - \Phi'^\dagger)_{be} (B)_{cf} \right] \end{aligned}$$

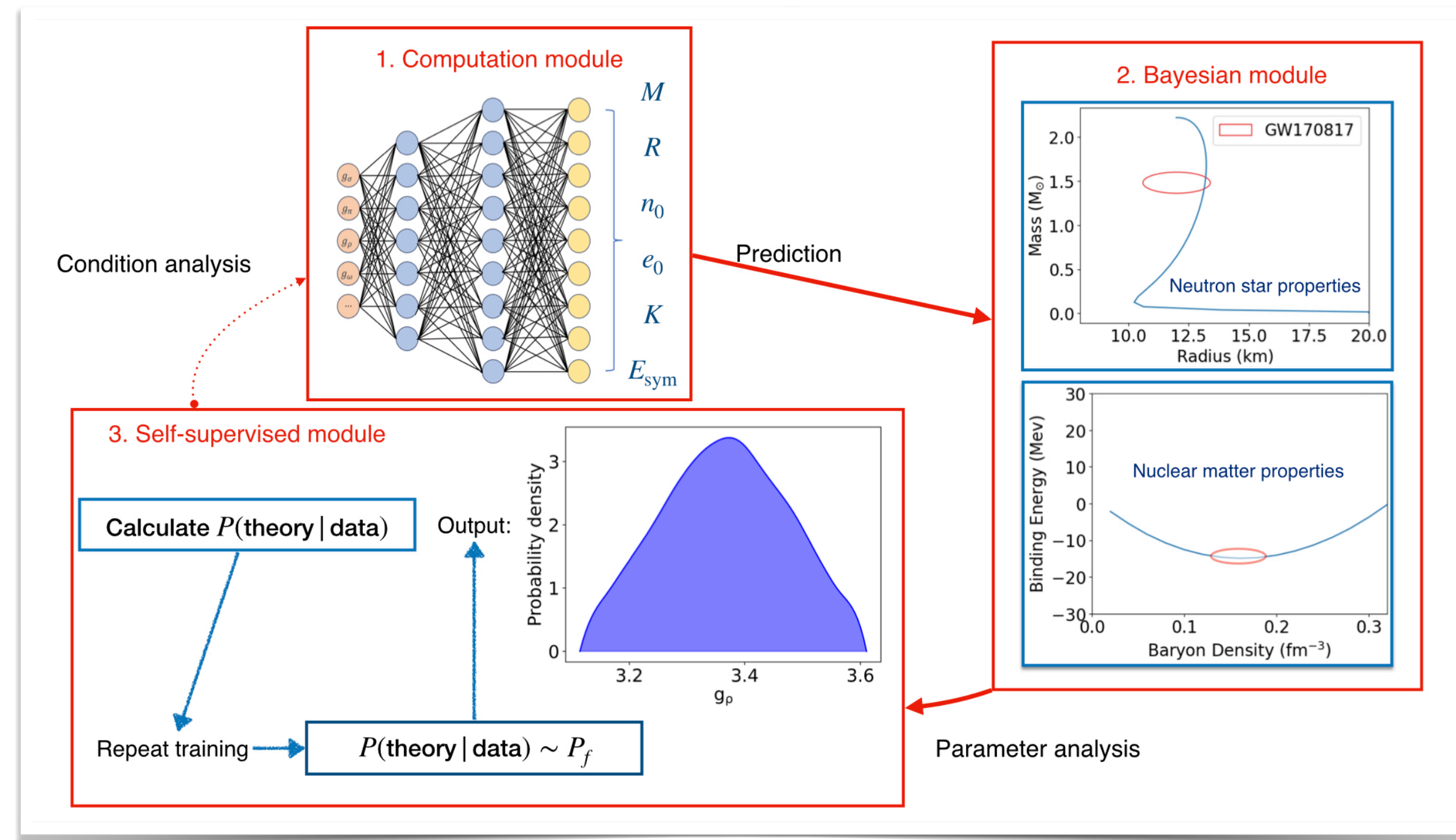
The baryon masses by spontaneous chiral symmetry breaking

Massive data processing (ML methods)

L.-J. Guo, J.-Y. Xiong, YM, and Y.-L. Ma, *Astrophys. J.* 965, 47 (2024)



- The parameter space searching of an EFT with data across broad scale is a rather labor- and time-consuming work
- AI techs based on machine learning have advantage to analysis massive data and statistical correlations



An application

$$\mathcal{L}_{\text{RMF}} = \bar{\psi} \left[i\gamma_{\mu} \partial^{\mu} - M - g_{\sigma} \sigma - g_{\omega} \gamma_{\mu} \omega^{\mu} - g_{\rho} \gamma_{\mu} \tau_a \rho^{a\mu} \right] \psi$$

$$+ \frac{1}{2} \partial_{\mu} \sigma \partial^{\mu} \sigma - \frac{1}{2} m_{\sigma}^2 \sigma^2 - \frac{1}{3} g_2 \sigma^3 - \frac{1}{4} g_3 \sigma^4$$

$$- \frac{1}{4} W_{\mu\nu} W^{\mu\nu} + \frac{1}{2} m_{\omega}^2 \omega_{\mu} \omega^{\mu} + \frac{1}{4} c_3 \left(\omega_{\mu} \omega^{\mu} \right)^2$$

$$- \frac{1}{4} R_{\mu\nu}^a R^{a\mu\nu} + \frac{1}{2} m_{\rho}^2 \rho_{\mu}^a \rho^{a\mu}$$

Y. Sugahara and H. Toki, Nucl. Phys. A 579, 557 (1994)

H. Shen, H. Toki, K. Oyamatsu, and K. Sumiyoshi, Nucl. Phys. A 637, 435 (1998)

TABLE II. Optimal values of the parameters calculated from NN. The empirical values $M_N = 938$ MeV, $m_{\omega} = 782$ MeV and $m_{\rho} = 765$ are physical values at vacuum taken as inputs from Ref. [68] for simplicity.

g_{σ}	g_{ω}	g_{ρ}	g_3	c_3	g_2	m_{σ}
9.82	11.8	3.42	1.26	72.6	-1550 MeV	531 MeV

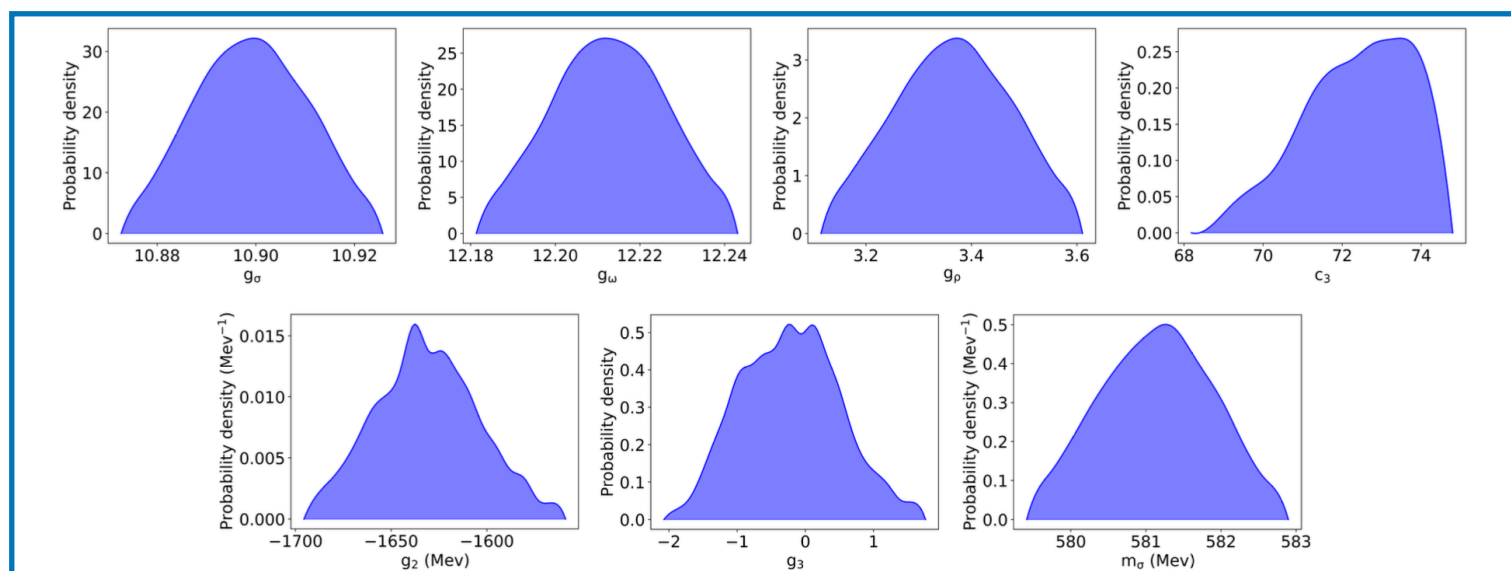


FIG. 5. Distributions of the parameters estimated by NN.

TABLE I. M and R is the mass and radius of the primary star in GW170817. e_0 is the binding energy of nucleon, $E_{\text{sym}}(n) = \frac{1}{2} \frac{\partial^2 E(n, \alpha)}{\partial \alpha^2} \Big|_{\alpha=0}$ is the symmetry energy and $K_0 = 9n_0^2 \frac{\partial^2 E(n, 0)}{\partial n^2} \Big|_{n=n_0}$ is the incompressibility coefficient at n_0 , respectively. Normal distribution is assumed for data error bars with 95% confidence level.

	$M (M_{\odot})$	R (km)	n_0 (fm^{-3})	e_0 (MeV)	E_{sym} (MeV)	K_0 (MeV)
Constraints	1.48 ± 0.12	11.9 ± 1.4	0.155 ± 0.05	-16 ± 1.0	32.0 ± 2.0	250 ± 50
Optimal	—	—	0.161	-15.7	28.6	266

Bayesian analysis

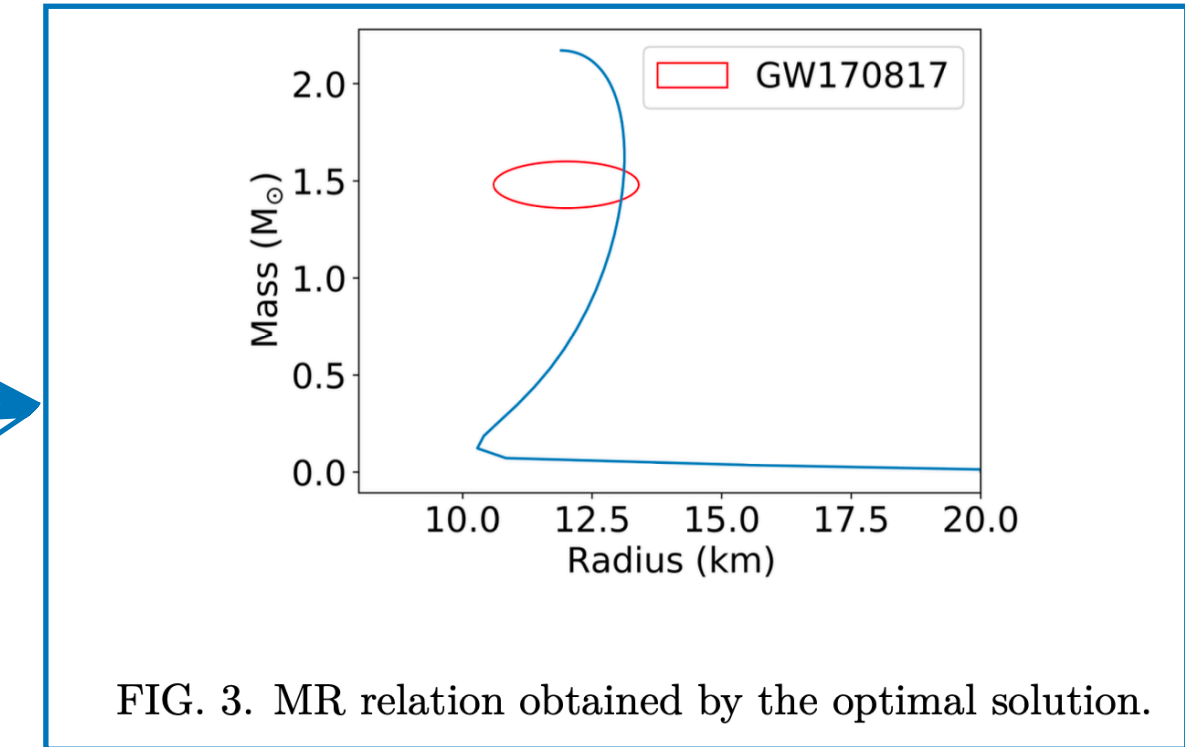


FIG. 3. MR relation obtained by the optimal solution.

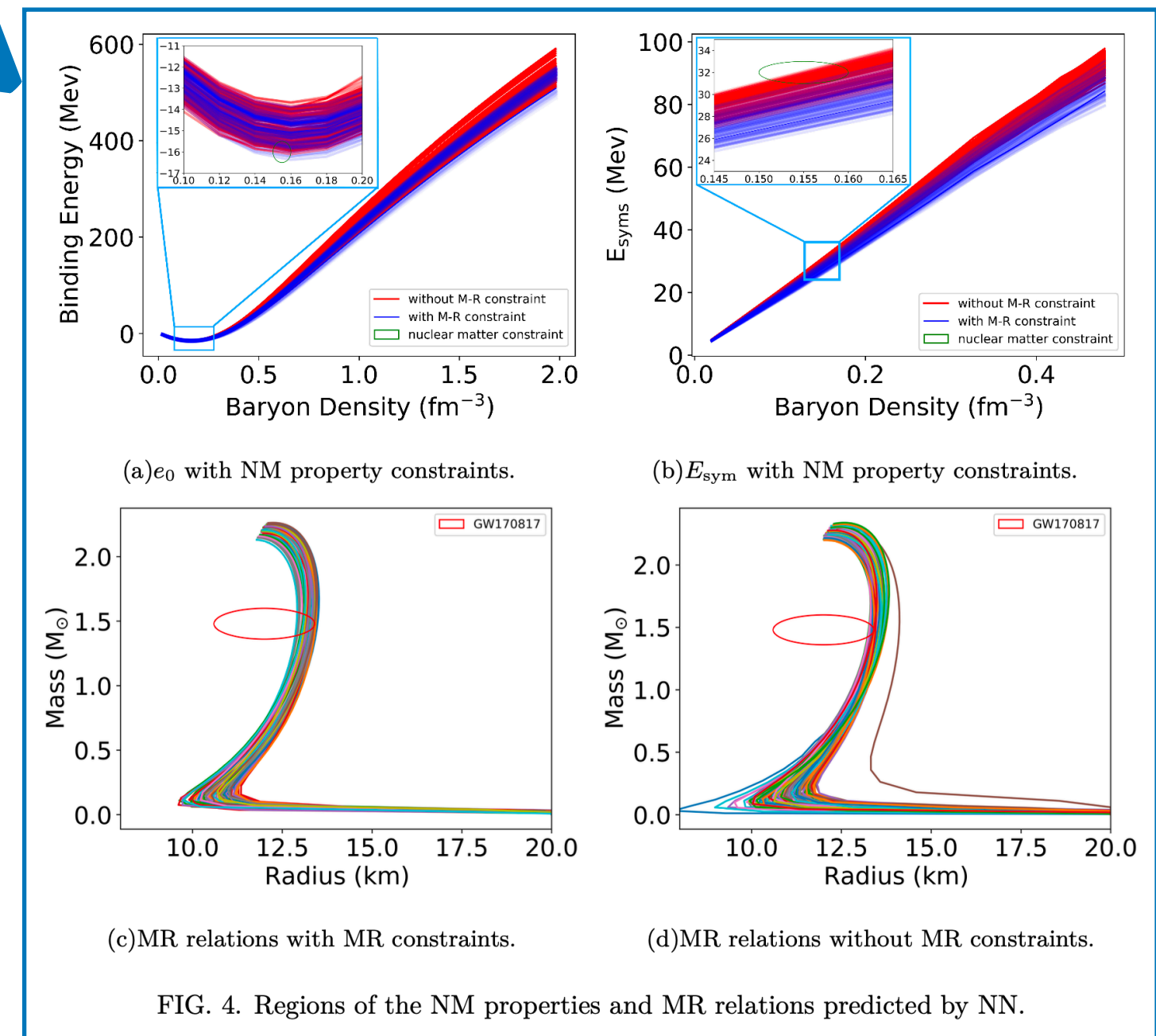


FIG. 4. Regions of the NM properties and MR relations predicted by NN.

An analysis on a more general Lagrangian

In collaboration with Ling-Jun Guo (郭凌君) and Jia-Ying Xiong(熊佳颖)



Include all possible operators contributing to RMF EOS up to dimension 4

$$\mathcal{L}_N = \bar{\Psi} \left(i\gamma^\mu \partial_\mu - m_N \right) \Psi,$$

$$\mathcal{L}_\sigma = \frac{1}{2} \left(\partial_\mu \sigma \partial^\mu \sigma - m_\sigma^2 \sigma^2 \right) - \frac{1}{3} g_2 \sigma^3 - \frac{1}{4} g_3 \sigma^4 - \frac{1}{2} g_4 \sigma^2 \omega^\mu \omega_\mu - \frac{1}{2} g_5 \sigma^2 \vec{\rho}^\mu \cdot \vec{\rho}_\mu - g_6 \sigma \vec{\rho}^\mu \cdot \vec{\rho}_\mu - g_7 \sigma \omega^\mu \omega_\mu,$$

$$\mathcal{L}_\omega = -\frac{1}{4} \Omega^{\mu\nu} \Omega_{\mu\nu} + \frac{1}{2} m_\omega^2 \omega^\mu \omega_\mu + \frac{1}{4} c_3 \left(\omega^\mu \omega_\mu \right)^2 + \frac{1}{2} c_4 \omega^\mu \omega_\mu \vec{\rho}^\mu \cdot \vec{\rho}_\mu$$

$$\mathcal{L}_\rho = -\frac{1}{4} \vec{P}^{\mu\nu} \cdot \vec{P}_{\mu\nu} + \frac{1}{2} m_\rho^2 \vec{\rho}^\mu \cdot \vec{\rho}_\mu + \frac{1}{4} d_3 \left(\vec{\rho}^\mu \cdot \vec{\rho}_\mu \right)^2$$

$$\begin{aligned} \mathcal{L}_{a_0} = & \frac{1}{2} \partial_\mu \vec{a}_0 \cdot \partial^\mu \vec{a}_0 - m_{a_0}^2 \vec{a}_0 \cdot \vec{a}_0 + \frac{1}{4} b_3 \left(\vec{a}_0 \cdot \vec{a}_0 \right)^2 + \frac{1}{2} b_4 \left(\vec{a}_0 \cdot \vec{a}_0 \right) \left(\vec{\rho}^\mu \cdot \vec{\rho}_\mu \right) + \frac{1}{2} b_5 \sigma \left(\vec{a}_0 \cdot \vec{a}_0 \right) \\ & + \frac{1}{2} b_6 \vec{a}_0 \cdot \vec{a}_0 \sigma^2 + \frac{1}{2} b_7 \vec{a}_0 \cdot \vec{a}_0 \omega^\mu \omega_\mu + b_8 \vec{a}_0 \cdot \vec{\rho}^\mu \omega_\mu \sigma + b_9 \vec{a}_0 \cdot \vec{\rho}_\mu \omega^\mu, \end{aligned}$$

$$\mathcal{L}_I = \bar{\Psi} \left(-g_\sigma \sigma - g_\omega \gamma^\mu \omega_\mu - g_\rho \gamma^\mu \vec{\rho}_\mu - g_{a_0} \vec{a}_0 \right) \Psi$$

$$\mathcal{L} = \mathcal{L}_N + \mathcal{L}_\sigma + \mathcal{L}_\omega + \mathcal{L}_\rho + \mathcal{L}_{a_0} + \mathcal{L}_I$$